Two-Dimensional Modeling and Analysis of Generalized Random Mobility Models for Wireless Ad Hoc Networks

Denizhan N. Alparslan and Khosrow Sohraby
School of Computing and Engineering
University of Missouri-Kansas City
5100 Rockhill Road
Kansas City, MO 64110-2499 USA
{dna5a0,sohrabyk}@umkc.edu

***Abstract*— Most of the important characteristics of wireless ad hoc networks such as link distance distribution, connectivity, network capacity, etc., is a consequence of the long-run properties of the mobility profiles of communicating terminals. Therefore, the analysis of the mobility models proposed for these networks becomes crucial. The contribution of this paper is to provide an analytical framework that is generalized enough to perform the analysis of realistic random movement models over two-dimensional regions. The synthetic scenarios that can be captured include hotspots where mobiles accumulate with higher probability and spend more time, and displacement dependent speed distributions. From the utilization of the framework to random waypoint mobility model, we derive an approximation to spatial distribution of terminals over rectangular regions. We validate the accuracy of this approximation via simulation, and by comparing the marginals with proven results for one-dimensional regions point out that it is insensitive to the proportion between dimensions of the terrain. In addition, we establish an example that demonstrates the applicability of the results derived to a scenario where mobile terminals are restricted to move on predefined paths, and provided long-run distributions by closed form expressions.**

***Index Terms*— Mobility Modeling, Long-Run Analysis, Ad Hoc Networks, Two-Dimensional Regions.**

I. Introduction

IN WIRELESS ad hoc networks communicating terminals move with respect to many different mobility patterns each one having unique attributes. Therefore, mobility modeling and its analysis becomes very important for the performance evaluation of these kinds of networks. In this paper, we focus on the long-run location and speed distribution analysis of a generalized random mobility modeling approach over two-dimensional mobility terrains.

The modeling methodology we are concentrating on is originally defined in [1] as a generalized model that is flexible enough to capture the major characteristics of several realistic movement profiles. In that paper, long-run location and and speed distributions are given in closed form expressions for one-dimensional regions. Here, we extend the analysis to two-dimensional terrains. A variety of examples are also given to show how the proposed model and its long-run analysis framework works for a broad range of mobility modeling approaches.

In what follows, we give a brief description of the generalized random mobility characterization approach that is analyzed in this article. Let R denote the two-dimensional closed region on which mobile terminals operate. A mobile located at the point $X_s = (X_{s_1}, X_{s_2}) \in R$, selects a random point $X_d = (X_{d_1}, X_{d_2}) \in R$ as destination according to the conditional probability density function (pdf) $f_{X_d|X_s}(x_d|x_s)$, and moves to point X_d on the straight line segment joining the two points, and at a speed V that is drawn randomly from the interval $[v_{min}, v_{max}]$, where $v_{min} > 0$, according to the conditional pdf $f_{V|X_s,X_d}$. After reaching the destination, mobile pauses for a random amount of time, denoted by T_p, at X_d, which is distributed with respect to the conditional pdf $f_{T_p|X_d}$, and whole cycle is repeated by selecting a new destination. Hence, the pattern of a mobile terminal is composed of consecutive movement epochs between the randomly selected points X_s and X_d, and it is uncorrelated with the movement behaviors of other terminals. Throughout this paper, we use the triplet $< f_{X_d|X_s}, f_{V|X_s,X_d}, f_{T_p|X_d} >$ to characterize the movement pattern of a mobile that moves with respect to this model.

Among the parameters of the triplet $< f_{X_d|X_s}, f_{V|X_s,X_d}, f_{T_p|X_d} >$, the conditional pdf $f_{X_d|X_s}$, which identifies the distribution of X_d given X_s at the embedded points in time where a new movement epoch starts. Incorporation of this kernel into this mobility characterization methodology provides the ability to define hotspots on the two dimensional mobility terrain where mobiles accumulate with higher probability, and correlations between consecutive hotspot decisions can be successfully modeled. Furthermore, since V is randomly drawn from $f_{V|X_s,X_d}$, we have the flexibility of constructing a correlation between the distribution of V and the locations of the starting point X_s and destination X_d. For instance, a scenario that identifies V proportional to the distance that is going to be traveled, that is, $|X_s - X_d|$, can be easily defined. In addition, the usage of $f_{T_p|X_d}$ makes it possible to capture different pause distributions at different destinations available for the mobility model.

For wireless ad hoc networks, there have been proposed a number of different mobility models. Comprehensive surveys of these models can be found in [2], [3]. Among them, the

random waypoint model [4] is one of the most widely used one for analytic and simulation-based performance analysis of ad hoc networks. In this model, a mobile selects a destination point in the mobility terrain with equal probability, and moves to that point with a speed that is drawn uniformly from a given range. After reaching the destination, mobile pauses for a random time, which has a distribution that is independent from the current location, and whole cycle is repeated by selecting a new destination. In [5], [6], [7], analytical frameworks are presented for the long-run analysis of this mobility model. The analysis that we propose in this paper is also applicable to random waypoint model, and to demonstrate the correctness and superiority of our work, we present a comparison of the results derived with the ones presented in literature.

The rest of this paper is outlined as follows. In Section II, we describe analytical framework we developed for long-run analysis. Section III provides the long-run distributions for a limited version of the exact mobility formulation constructed according to the methodology explained in the second section. Section IV extends the results derived in section three and provides the distributions for the generalized model proposed. In Section V, we focus on example scenarios, and the final section presents a summary of the paper.

II. Methodology and Description of Analytical Framework

In this section, we describe the analytical framework we establish for the long-run analysis of the generalized mobility model proposed.

Now since the movement behavior of mobiles are assumed to be uncorrelated with each other, we can concentrate on a single terminal for long-run analysis. Hence, for the terminal whose movement pattern is characterized by the triplet $< f_{X_d|X_s}, f_{V|X_s,X_d}, f_{T_p|X_d} >$, let the vector $\mathbf{X}(t)$ denote the state descriptor whose components identify the current location, destination, and the speed of that mobile at time t. In our solution methodology, we discretisize the two-dimensional mobility terrain R and approximate the random variable V with a discrete random variable so that the stochastic process $\{\mathbf{X}(t), t \geq 0\}$ can be defined on a multidimensional discrete state space. The assumptions that we have made to generate this discrete state space are as follows:

A_1: The closed region R is discretisized into n disjoint, non-overlapping cells of the same shape denoted by c_i, $i = 0 \ldots n-1$, such that $R \subseteq \bigcup_{i=0}^{n-1} c_i$ where $n > 1$. A mobile terminal is assumed to occupy one of the c_i's at any moment in time, and movement epochs occur between two randomly picked starting and destination cells.

A_2: The random variable V, that is, the speed during a movement epoch, is approximated by the discrete random variable V^* defined on the state space $\mathcal{S}_{V^*} = \{z_1, z_2, \ldots, z_m\}$ where $z_r = r\,\Delta v$, $r = 1, \ldots, m$, for some discretization parameter $\Delta v > 0$, and an integer $m \geq 1$ such that $\Delta v \leq v_{\min}$ and $v_{max} = m\Delta v$.

Based on these assumptions, observe that a mobile can be in pausing or moving modes at the cell it is currently located.

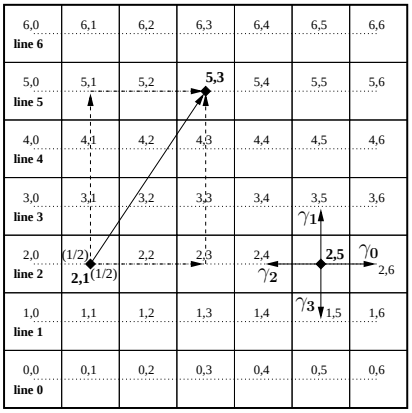

Fig. 1. Discretization of the square region R into squares.

Additionally, instead of observing the state of a terminal continuously, we observe it at embedded times denoted by T_k, for $k \in \mathbf{N}$, such that $T_0 = 0,\ T_{k+1} \geq T_k,\ \forall k \in \mathbf{Z}^+$, which point to the time of occurrence of one of the following events:

E_1: The terminal which is in pause mode, selects a new cell as destination that is different from the current cell occupied, and changes its state to moving state in the current cell it is located,

E_2: The terminal which is traveling in the direction of the target cell, moves out from the current cell and enters the neighboring cell that lies on the shortest path between the current and destination cells,

E_3: The terminal reaches to the destination cell and enters the pause mode at that location.

At this point, notice that the discretization of the two-dimensional region R into n cells of the same shape, such that every point in R belongs to one cell, can performed through the use of triangles, parallelograms (including squares and rectangles), or hexagons. We note that, the idea of dividing the region on which mobile terminals operate to regular polygons of the same shape has been generally used by some studies concentrating on the performance analysis of cellular networks. For instance, the studies presented in [8] and [9], assume radio coverage of a base station to be a hexagon or a square, and present a performance analysis study that is done with respect to a mobility model which formulates the movement behavior of the terminals between those cells on a macroscopic scale. However, in our analysis, we discretisize the region R on a microscopic scale to approximate the exact location that can be occupied by a terminal at any point in time. On the other hand, in the performance modeling of cellular networks, the exact location of a terminal inside the coverage area of a base station is not the main issue, and the main problem is to identify the base station that it is attached to.

In our analysis, to apply assumption A_1, we focus on the discretization methods that partition the region R into squares or hexagons. The reasoning behind concentrating on two different discretization approaches for R concurrently will become more clear as we proceed further in the long-run

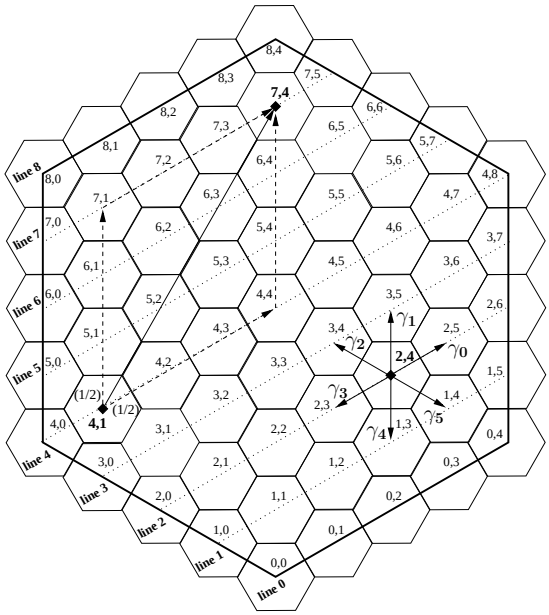

Fig. 2. Discretization of the hexagonal region R into hexagons.

analysis. In Fig. 1 and Fig. 2, we applied these discretization approaches to square and hexagonal regions. It should be also noted that, in principle, any closed region can be discretisized by squares or hexagons. Here we decided to discretisize a square with squares, and a hexagon with hexagons because we wanted the discretization technique to be consistent with the shape of the region.

In Fig. 1 and Fig. 2, we also depicted the scheme we decided on to identify the cells on the discretisized region. Basically, the centers of the cells are grouped by lines that are parallel to each other, and the index i of cell c_i is denoted by $i = (\ell_i, \ell_i')$ where ℓ_i represents the line that the center of c_i is located, and ℓ_i' is its location on that line. For the rest of this paper, we will use the notations c_i and $c_{(\ell_i,\ell_i')}$ interchangeably. Hence, if there are n_ℓ lines, and if q_ℓ denotes the number of cells on line ℓ, then set of the cells on the discretisized region can be defined as follows:

$$\tilde{R} = \bigcup_{\ell=0}^{n_\ell-1} \{c_{(\ell,0)}, \ldots, c_{(\ell,q_\ell-1)}\}, \tag{1}$$

It should be noted that, as the side lengths of the discretization hexagons decreases, the total area covered by the union of the cells in $\tilde{R}$ becomes close to the area of R.

Clearly, the path traveled during a movement epoch described by the discretisized version of the mobility characterization we constructed, is composed of consecutive straight line segments between the centers of the cells c_i, $i = 0, \ldots, n-1$. In other words, a mobile terminal moves to one of the neighboring cells from the current cell occupied while traveling towards the destination cell. Hence, if d denotes the number of available movement directions for the discretisized mobility formulation, then d would be equal to the number of the sides of the regular polygons used in the discretization process. Thus, $d = 4$ for square discretization, and $d = 6$ for hexagonal discretization, and let $\gamma_\imath, \imath = 0, \ldots, d-1$ denote those directions (see cell $c_{(2,5)}$ in Fig. 1, and cell $c_{(2,4)}$ in Fig. 2). On the other hand, in principle, if there are no obstacles on the region R that can restrict the movement directions, then mobile should be able to move at any direction. Therefore, by discretizing the region, we are also forced to *discretisize the movement direction*. Obviously, if R is discretisized by regular polygons of the same shape, as we are doing, then d can be at most equal to six. Furthermore, if the discretization of a region R with a general shape (e.g. rectangle) with regular polygons is done for the purpose approximating the exact location of a terminal, as in our case, then using hexagons is a better choice because the number of available movement directions are higher, and a more realistic approximation can be done to the exact mobility pattern.

At this point, it should be noted that, the enforcement of discretizing movement directions will not arise for the one-dimensional case because there are only two directions for a mobile to move on a one-dimensional region and discretization method does not enforce any kind of restriction on these directions. Clearly the fundamental difference between the discretization parameters d, and n and m is that n and m can be increased, but d, as we have mentioned above, can be at most equal to six. This difference introduces a new issue that has to be clarified before continuing. In what follows, we explain this issue and our solution approach for it.

Now recall that according to our mobility model proposed, during a movement epoch, mobile travels on the straight line joining the points X_s and X_d. In the discretisized version of this mobility model, movement epochs occur between randomly selected cells. Obviously if the mobile terminal is allowed to move at any direction in the region R, then the shortest path between those two points is just the straight line between them, and it is unique. However, for the discrete formulation, the shortest path is defined in terms of the number of jumps between cells. More importantly, for a discretization that is done according to squares (i.e., $d = 4$), or to hexagons (i.e., $d = 6$), if $\tilde{p}^{(d)}(i,j)$, $d = 4, 6$, denotes the ordered list of the cells that are located on a shortest path for the movement epoch that had started at c_i, and ended up at destination cell c_j, then the members of $\tilde{p}^{(d)}(i,j)$ will not be necessarily unique. The algorithm that we use in this paper to generate $\tilde{p}^{(d)}(i,j)$ is as follows. If c_j is towards the direction $\gamma_{\imath'}$ for some $\imath' \in \{0, \ldots, d-1\}$ from c_i, then mobile follows that direction until it reaches destination c_j. On the other hand, mobile proceeds to the next cell either in the direction $\gamma_{\imath'}$ or $\gamma_{\imath'+1 \bmod d}$ with equal probabilities for some $\imath' \in \{0, \ldots, d-1\}$ that generates the least possible shortest path if selected, and continues in that direction until it reaches to a cell that can be joined to c_j by following one of the d available directions. For example, in Fig. 2, consider the scenario where $c_i = c_{(4,1)}$ and $c_j = c_{(7,4)}$. Observe that for this scenario, this algorithm either generates the path $\{c_{(4,1)}, c_{(4,2)}, c_{(4,3)}, c_{(4,4)}, c_{(5,4)}, c_{(6,4)}, c_{(7,4)}\}$ or the path $\{c_{(4,1)}, c_{(5,1)}, c_{(6,1)}, c_{(7,1)}, c_{(7,2)}, c_{(7,3)}, c_{(7,4)}\}$. A similar example can be also found in Fig. 1. It should be also noted that, according to our notation, the first and the last members of the list $\tilde{p}^{(d)}(i,j)$ are c_i and c_j, respectively.

Having clarified these issues, we now proceed to the formal definition of the discretisized mobility formulation. Denote $\mathbf{S}_k$,

$k \in \mathbf{N}$, as the state of the mobile terminal at time T_k. Hence, based on assumptions A_1, A_2, and the events E_1, E_2, E_3 that identify observation times T_k, for $k \in \mathbf{N}$, the finite-state space of $\mathbf{S}_k$ will be defined as follows:

$$\mathcal{S} = \mathcal{S}_{\mathcal{M}} \cup \mathcal{S}_{\mathcal{P}} \tag{2}$$

where

$$\mathcal{S}_{\mathcal{M}} = \{(c_i, c_j, z_r, q) \mid i, j = 0, \ldots, n-1, i \neq j, \\ r = 1, \ldots, m, q = 1\} \tag{3}$$

$$\mathcal{S}_{\mathcal{P}} = \{(c_i, q) \mid i = 0, \ldots, n-1, q = 0\} \tag{4}$$

where c_i is the current cell occupied, c_j is the destination cell, z_r is the discretisized speed, and q is the indicator function that is defined as follows:

$$q = \begin{cases} 1, & \text{mobile is moving towards the target cell} \\ 0, & \text{mobile is pausing at the destination cell} \end{cases} \tag{5}$$

Consequently, the stochastic process $\{\mathbf{X}(t), t \geq 0\}$ can be formally defined on the finite-state space $\mathcal{S}$ according to the following expression:

$$\mathbf{X}(t) = \mathbf{S}_k, \quad \text{if } T_k \leq t < T_{k+1}$$

Notice that when $\mathbf{X}(t)$ occupies a state $s \in \mathcal{S}_{\mathcal{M}}$, since the state s has a separate dimension for the destination cell, the next state to be visited can be determined from the components of it. In other words, the future evolution of the stochastic process $\{\mathbf{S}_k, k \in \mathbf{N}\}$ becomes dependent only on the current state of the mobile terminal, not on its history at previous observation points. Furthermore, for all $s \in \mathcal{S}$, the distribution of sojourn time in state s would be independent from the previous states occupied and can be determined only from the components of state s.

Therefore, the stochastic process $\{\mathbf{S}_k, T_k; k \in \mathbf{N}\}$ with finite-state space $\mathcal{S}$ satisfies the conditions for being *Markov Renewal Process*, and the process $\{\mathbf{X}(t), t \geq 0\}$ can be called as the *semi-Markov process* (SMP) associated with $\{\mathbf{S}_k, T_k; k \in \mathbf{N}\}$ [10]. Moreover, since the distributions for destination, speed, and pause time parameters are assumed to be *time-homogeneous* in the mobility model proposed, the distribution of state holding time in state s, given that the next state to be visited is s', would be independent of k. Hence, the transitions of the process $\mathbf{X}(t)$ at the embedded time instants T_k can be governed by the *discrete-time* Markov chain (DTMC) $\{\mathbf{S}_k, k \in \mathbf{N}\}$ with finite-state space $\mathcal{S}$ and transition probability matrix $P = [p_{s\,s'}]$, where $p_{s\,s'} = \Pr\{\mathbf{S}_{k+1} = s' \,|\, \mathbf{S}_k = s\}$, such that $\sum_{s' \in \mathcal{S}} p_{s\,s'} = 1$ for all $s \in \mathcal{S}$. The process $\{\mathbf{S}_k, k \in \mathbf{N}\}$ is also referred as *embedded* DTMC of SMP.

Thus, in order to characterize the SMP $\{\mathbf{X}(t), t \geq 0\}$ at the long-run, the DTMC $\{\mathbf{S}_k, k \in \mathbf{N}\}$ must satisfy the ergodicity conditions and the mean state holding times must be finite. If these conditions are satisfied, then the long-run proportion of time spent in a state $s \in \mathcal{S}$ can be obtained, and after aggregating the states that has the same *current cell* and *speed* components, the long-run distributions sought can be derived for this discretisized version of the mobility formulation.

Notice that, as the discretization parameters $n \to \infty$ and $m \to \infty$, we obtain better approximations to the location and speed of the mobile terminals, respectively, and in the limit we converge to a restricted version the continuous model where the available movement directions are limited by the d different directions $\gamma_0, \ldots, \gamma_{d-1}$ given by

$$\gamma_\imath = \begin{cases} \frac{2\pi\,\imath}{d}, & \text{if } d = 4, \\ \frac{2\pi\,(\imath+1/2)}{d}, & \text{if } d = 6, \end{cases} \tag{6}$$

for $\imath = 0, \ldots, d-1$. Visualization of these directions are also provided in Fig. 1 and 2. Clearly because of the methodology we decided to generate $\tilde{p}^{(d)}(i,j)$, at the limit $n \to \infty$, the path followed during a movement epoch between X_s and $X_d \in R$ will generally be composed of two directed finite line segments towards the directions $\gamma_{\imath_1}$ and $\gamma_{\imath_2}$ where $\{\imath_1 = \imath, \imath_2 = (\imath+1) \bmod d\}$ or $\{\imath_1 = (\imath+1) \bmod d, \imath_2 = \imath\}$ for some $\imath \in \{0, \ldots, d-1\}$. This can be also observed from the example movement scenarios depicted in Fig. 1 and 2. Obviously if X_d is towards any of directions $\gamma_\imath$, $\imath = 0, \ldots, d-1$, from X_s, then the path will be composed of a single straight line. For the rest of this report we will use the term *continuous-d mobility formulation* to refer to this limited version of the exact continuous mobility formulation. Finally, we note that, since d can be at most equal to six, a formal transition from this limited case to the original continuous formulation cannot be done. Therefore, in the following sections we will use distributions of the continuous-d mobility formulation to gain some insight into the distributions that can be conjectured for the original case.

III. Analytical Results for The Discretisized and Continuous-d Mobility Formulation

In this section, we first concentrate on generating the long-run location and speed distributions for the discretisized case, and after that we will use those results to derive long-run distributions of the continuous-d mobility formulation.

Now, to able to identify the transition probabilities of the DTMC $\{\mathbf{S}_k, k \in \mathbf{N}\}$, we first denote $\tau_{j|i}$ as the probability of selecting cell c_j as target from cell c_i. Then, according to the mobility characterization parameter $f_{X_d|X_s}$, $\tau_{j|i}$ will be given by

$$\tau_{j|i} = \int_{x_d \in c_j} f_{X_d|X_s}(x_d | X_s \in c_i)\, dx_d, \tag{7}$$

Similarly, denote $\nu_{r|i,j}$ as the conditional probability mass function of V^* for a movement epoch that had started at cell c_i with destination c_j. Then, by using the parameter $f_{V|X_s,X_d}$ we have

$$\nu_{r|i,j} = \int_{(r-1)\Delta v}^{r\Delta v} f_{V|X_s,X_d}(v | X_s \in c_i, X_d \in c_j)\, dv \tag{8}$$

for $r = 1, \ldots, m$. In addition, let $n_h(c_i)$ denote the cells in the neighborhood of cell c_i that can be reached in one jump from it, and let $[i', i, j]$ denote the index of the cell $c_{i'}$ in the ordered list that defines the path $\tilde{p}^{(d)}(i,j)$. Note that, $[i, i, j] = 1$, and $[j, i, j] = \left\|\tilde{p}^{(d)}(i,j)\right\|$ where $\left\|\tilde{p}^{(d)}(i,j)\right\|$ denotes the number of the cells on the path $\tilde{p}^{(d)}(i,j)$. Hence, if we are interested in the probability of the cell $c_{i'}$ to be the next cell to be visited after cell c_i, that is, $\Pr\{[i', i, j] = 2\}$, then $\Pr\{[i', i, j] = 2\}$ is either equal to 1, or $1/2$, or 0 (i.e. $c_{i'}$ is not on the path

TABLE I

TRANSITION PROBABILITIES OF THE PROCESS $\{\mathbf{S}_k, k \in \mathbf{N}\}$

Event	Transition	Probability	Condition*
E_1	$(c_i,0) \rightarrow (c_i,c_j,z_r,1)$	$\frac{\tau_{j\|i}}{1-\tau_{i\|i}}\nu_{r\|i,j}$	$i \neq j$
E_2	$(c_i,c_j,z_r,1) \rightarrow (c_{i'},c_j,z_r,1)$	1	$c_j \notin n_h(c_i)$, $\Pr\{[i',i,j]=2\} = 1$
		1/2	$c_j \notin n_h(c_i)$, $\Pr\{[i',i,j]=2\} = 1/2$
E_3	$(c_i,c_j,z_r,1) \rightarrow (c_j,0)$	1	$c_j \in n_h(c_i)$

* $i,i',j = 0,\ldots,n-1, \quad r = 1 \ldots m$

$\tilde{p}^{(d)}(i,j)$). For instance, in Fig. 2, when $c_i = c_{(4,1)}$, $c_j = c_{(7,4)}$, and $c_{i'} = c_{(4,2)}$, then $\Pr\{[i',i,j]=2\} = 1/2$. On the other hand, if $c_i = c_{(4,1)}$, $c_j = c_{(4,4)}$, and $c_{i'} = c_{(4,2)}$, then $\Pr\{[i',i,j]=2\} = 1$.

Based on these definitions, the transition probabilities corresponding to the events E_1, E_2, and E_3, can be grouped as in Table I.

Next, we examine the irreducibility and aperiodicity of the DTMC $\{\mathbf{S}_k, k \in \mathbf{N}\}$ with respect to the transition probabilities defined in Table I. Let φ_i denote the probability of starting a movement epoch from a cell c_i, $i = 0,\ldots,n-1$ at the steady-state. Obviously, in order to satisfy the irreducibility, φ_i must be greater than 0 for all $i = 0,\ldots,n-1$. Otherwise, some cells on the two-dimensional discretisized region will never be visited (i.e., selected as destination) and the chain becomes reducible. Hence, a steady-state distribution must exist for X_s. The conditional pdf $f_{X_d|X_s}(x_d|x_s)$, which identifies the distribution of X_d given X_s at the embedded points in time where a new epoch starts, is referred as *stochastic density kernel* by Feller [11]. Under some "mild" regularity conditions defined in [11] on $f_{X_d|X_s}(x_d|x_s)$ the steady-state distribution of X_s with pdf $f_{X_s}(x_d)$ can be uniquely determined from the solution of the following integral equation

$$f_{X_s}(x_d) = \int_{x_s \in R} f_{X_d|X_s}(x_d|x_s) f_{X_s}(x_s) dx_s, \qquad (9)$$

and φ_i will then be equal to

$$\varphi_i = \int_{x_d \in c_i} f_{X_s}(x_d)\, dx_d \qquad (10)$$

Observe that, if $T = [\tau_{j|i}]$, and if the integral equation (9) has a unique solution, then φ_i can be also obtained by solving $\varphi T = \varphi$, $\|\varphi\|_1 = 1$ where $\varphi = [\varphi_0,\ldots,\varphi_{n-1}]$.

In view of the discussions above, we state the following result.

Lemma 1: If the p.d.f. $f_{X_s}(x_d)$ can be uniquely determined from the solution of the integral equation (9), and if $\nu_{r|i,j} > 0$, $i,j = 0,\ldots,n-1$ and $r = 1,\ldots,m$, then the embedded DTMC $\{\mathbf{S}_k, k \in \mathbf{N}\}$ defined on state space $\mathcal{S}$ in (2), with transition probabilities given as in Table I, is irreducible and aperiodic.

Proof: Refer to Appendix II. ■

Next, we provide the steady-state distribution of the DTMC $\{\mathbf{S}_k, k \in \mathbf{N}\}$. Using Lemma 1, and a direct substitution approach that does not require to define the transition probability matrix of this DTMC in full generality, we reach to the following:

Lemma 2: For the DTMC $\{\mathbf{S}_k, k \in \mathbf{N}\}$ defined on the state space $\mathcal{S}$ in (2), where d is either equal four or six, let $\pi_i^{(d)}$ and $\pi_{(i,j,r)}^{(d)}$ denote the steady-state probabilities of being in the states of the form $s = (c_i,0),\ i = 0,\ldots,n-1$, and $s = (c_i,c_j,z_r,1),\ i,j = 0,\ldots,n-1,\ i \neq j, r = 1,\ldots,m$, respectively. If the conditions of Lemma 1 are satisfied, then they are uniquely given by

$$\pi_i^{(d)} = \varphi_i\,(1-\tau_{i|i})/N, \qquad (11)$$

$$\boldsymbol{\pi}_{i,j}^{(d)} = \sum_{c_{i'} \in p_{t,1}^{(d)}(i,j)} \varphi_{i'}\ \tau_{j|i'}\ \boldsymbol{\nu}_{m|i',j}/N + \tfrac{1}{2} \sum_{c_{i'} \in p_{t,2}^{(d)}(i,j)} \varphi_{i'}\ \tau_{j|i'}\ \boldsymbol{\nu}_{m|i',j}/N \qquad (12)$$

where

$$\boldsymbol{\pi}_{i,j}^{(d)} = [\pi_{(i,j,1)}^{(d)},\ldots,\pi_{(i,j,m)}^{(d)}], \qquad (13)$$

$$\boldsymbol{\nu}_{m|i',j} = [\nu_{1|i',j},\ldots,\nu_{m|i',j}], \qquad (14)$$

and

$$p_{t,1}^{(d)}(i,j) = \left\{c_{i'} | c_{i'} \in \tilde{R}, \Pr\{c_i \in \tilde{p}^{(d)}(i',j)\} = 1\right\}, \qquad (15)$$

$$p_{t,2}^{(d)}(i,j) = \left\{c_{i'} | c_{i'} \in \tilde{R}, \Pr\{c_i \in \tilde{p}^{(d)}(i',j)\} = 1/2\right\}, \qquad (16)$$

and $N = \sum_{i=0}^{n-1} \pi_i^{(d)} + \sum_{i=0}^{n-1} \sum_{\substack{j=0,\\ j\neq i}}^{n-1} \left\|\boldsymbol{\pi}_{i,j}^{(d)}\right\|_1$.

Proof: Refer to Appendix II. ■

It should be noted that, the sets $p_{t,1}^{(d)}(i,j)$ in (15) and $p_{t,2}^{(d)}(i,j)$ in (16) represent the subset of cells in $\tilde{R}$ from where a movement epoch originated with destination cell c_j passes through the cell c_i with probabilities 1 and 1/2, respectively.

Now, let $\bar{t}_s$ denote the sojourn time of the SMP $\{\mathbf{X}(t), t \geq 0\}$ in state $s \in \mathcal{S}$. Then, if $s = (c_i,c_j,z_r,1)$ (i.e., mobile is moving towards the destination with discrete speed z_r), and if $\Delta c^{(d)}$ denotes the traveled distance in a cell while passing trough it, then

$$\bar{t}_s = \frac{\Delta c^{(d)}}{z_r} \qquad (17)$$

Notice that, if the discretization is done with squares of side length Δs, then, $\Delta c^{(4)} = \Delta s$, and if it is done with respect to the hexagons of side length Δh, then $\Delta c^{(6)} = \sqrt{3}\Delta h$. On the other hand, if $s = (c_i,0)$, then we define the following.

$$\bar{t}_s = E[T_{p_i}] = E[T_p | X_s \in c_i] = \int_0^\infty \Pr\{T_p > t_p | X_s \in c_i\}\, dt_p \qquad (18)$$

Finally, in order to characterize the SMP $\{\mathbf{X}(t), t \geq 0\}$ at the long-run, the following must be satisfied [10]:

$$\sum_{s \in \mathcal{S}} \pi_s \bar{t}_s < \infty \qquad (19)$$

Hence, by applying the theory of semi-Markov processes we obtained the long-run proportion of time that the SMP $\{\mathbf{X}(t), t \geq 0\}$ is in a state $s \in \mathcal{S}$. After aggregating the states in $\mathcal{S}$ that has the same *current location* and *speed* components,

including the ones with zero speed (i.e, $s = (c_i, 0)$), we reach to the following result.

Lemma 3: For the mobile terminal, whose mobility pattern is characterized according to the discretisized version of the $< f_{X_d|X_s}, f_{V|X_s,X_d}, f_{T_p|X_d} >$ mobility formulation, let $p_i^{(d)}$, $i = 0, \ldots, n-1$, $d = 4, 6$, denote the long-run proportion of time that terminal stays in cell c_i, which can be a square or hexagon. Similarly, denote $\psi_r^{(d)}$ as the long-run proportion of time that mobile possesses speed $z_r = r\delta v$, $r = 0, \ldots, m$. If the conditions given by Lemma 1 are satisfied, and equation (19) holds to be true, then

$$p_i^{(d)} = \frac{\varphi_i \left(1 - \tau_{i|i}\right) E[T_{p_i}] + \sum_{r=1}^{m} k_{i,r}^{(d)}}{N_{n,m}^{(d)}}, \tag{20}$$

and

$$\psi_r^{(d)} = \begin{cases} \sum_{i=0}^{n-1} \varphi_i \left(1 - \tau_{i|i}\right) E[T_{p_i}] \, / N_{n,m}^{(d)} \, , & \text{if } r = 0 \\ \sum_{i=0}^{n-1} k_{i,r}^{(d)} / N_{n,m}^{(d)} \, , & \text{else} \end{cases} \tag{21}$$

where

$$k_{i,r}^{(d)} = \sum_{c_j \in \tilde{R} - \{c_i\}} \Big(\sum_{c_{i'} \in p_{t,1}^{(d)}(i,j)} \varphi_{i'} \tau_{j|i'} \frac{1}{z_r} \, \nu_{r|i',j} \, \Delta c^{(d)} + \tfrac{1}{2} \sum_{c_{i'} \in p_{t,2}^{(d)}(i,j)} \varphi_{i'} \tau_{j|i'} \frac{1}{z_r} \, \nu_{r|i',j} \, \Delta c^{(d)} \Big), \tag{22}$$

and

$$N_{n,m}^{(d)} = \sum_{i=0}^{n-1} \varphi_i \left(1 - \tau_{i|i}\right) E[T_{p_i}] + \hat{D}_n^{(d)} \tag{23}$$

where

$$\hat{D}_n^{(d)} = \sum_{i=0}^{n-1} \sum_{r=1}^{m} k_{i,r}^{(d)} \tag{24}$$

To simplify the formulation of $\hat{D}_n^{(d)}$ in (24) for some special cases, we now state the following claim.

Claim 1: If the distribution of V^* is assumed to be independent from the location of the starting and destination cells of the movement epochs, the expression for $\hat{D}_n^{(d)}$ in (24) is equivalent to the following:

$$\hat{D}_n^{(d)} = E[\frac{1}{V^*}] \sum_{c_i \in \tilde{R}} \sum_{c_j \in \tilde{R}} \varphi_i \; \tau_{j|i} \; dis^{(d)}(i,j) \; \Delta c^{(d)}, \tag{25}$$

where $dis^{(d)}(i,j) = \left\| \tilde{p}^{(d)}(i,j) \right\| - 1$, that is, the number of the discrete jumps made on the path $\tilde{p}^{(d)}(i,j)$.

Proof: Refer to Appendix II. ∎

Before continuing on with the long-run analysis of the continuous-d mobility formulation, in order to clarify the interpretation of term $k_{i,r}^{(d)}$ given in (22), we now concentrate on a simple example scenario. Now, consider a continuous mobility formulation (i.e., mobiles can move anywhere at any direction) over the region $R = [0, a] \times [0, a]$ where V is deterministic and equal v, and the other mobility characterization parameters, $f_{X_d|X_s}$ and $f_{T_p|X_d}$, can be arbitrary as long as the integral equation in (9) is uniquely solvable and equation (19) is satisfied. Now to be able to apply Lemma 3, we need to generate the discretisized version of this mobility formulation. Hence, assume $n = 4$, $d = 4$, and since V is deterministic, $m = 1$. In Fig. 3 we provided a visualization of the discretisized mobility model generated according to these assumptions.

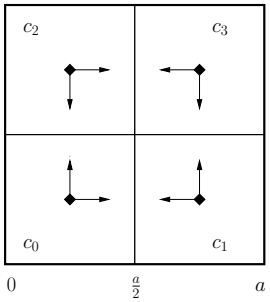

Fig. 3. Discretisized version of a simple mobility scenario ($n = 4$, $d = 4$).

Now for this discretisized mobility formulation, if we are interested in the long-run proportion of time mobile stays in cell c_0 (i.e., $p_0^{(4)}$), then according to Lemma 3 we simply have

$$p_0^{(4)} = \frac{\varphi_0 \left(1 - \tau_{0|0}\right) E[T_{p_0}] + k_{0,1}^{(4)}}{N_{4,1}^{(4)}}, \tag{26}$$

where

$$k_{0,1}^{(4)} = \frac{a}{2v}(\varphi_0 \tau_{1|0} + \tfrac{1}{2}\varphi_2 \tau_{1|2} + \varphi_0 \tau_{2|0} + \tfrac{1}{2}\varphi_1 \tau_{2|1} + \varphi_0 \tau_{3|0}), \tag{27}$$

which is equal to the average time spent over the cell c_0 while moving between randomly picked cells. In other words, $k_{0,1}^{(4)}$ is equal to $\frac{a/2}{v}$ multiplied with the probability of a movement epoch between two randomly picked cells to pass trough the cell c_0, including the ones starting or ending at cell c_0. Notice that in this simple formulation $\nu_{r|i',j} = 1$ for all $i', j = 0, \ldots, 3$. However, if the distribution of V is dependent on X_s and X_d in the original continuous mobility formulation, then $m > 1$, and we have to multiply each additive term of $k_{0,r}^{(4)}$, $r = 1, \ldots, m$ with the probability of selecting speed $z_r = r\delta v$, (i.e., $\nu_{r|i',j}$) and $\frac{1}{z_r}$ for the the movement epoch that passes trough cell c_0, as it is shown by the formulation of $k_{i,r}^{(d)}$ in (22). Observe that, for all choices of V, the term $\sum_{r=1}^{m} k_{i,r}^{(d)}$ corresponds to the expected time spent over cell c_i while moving between two randomly picked cells that are drawn from the distributions $\varphi_{i'}$ in (10) and $\tau_{j|i'}$ in (7), respectively.

Next we proceed to the long-run analysis of the continuous-d mobility formulation. At first, recall that in this case since movement directions are restricted to 4 or 6 different directions, the path followed during a movement epoch between the points $X_s \in R$ and $X_d \in R$ will be composed two or one line segments each directed towards one of the available directions $\gamma_\imath$ in (6), $\imath = 0, \ldots, d-1$. Thus, in order to keep the formulation of this case separate from the exact case, where movement epochs occur on a single directed line segment that can have any direction, let the random variables $X^{(d)}(t) = (X_1^{(d)}(t), X_2^{(d)}(t))$ and $\tilde{V}^{(d)}(t)$, where d is either 4

or 6, denote the location and the speed of a mobile terminal at time t, respectively. Note that $X^{(d)}(t) \in R$, and since the mobile can be in moving or pausing modes at any point in time, $\tilde{V}^{(d)}(t)$ is either equal to 0, or in the range $[v_{min}, v_{max}]$.

Now let $X^{(d)} = (X_1^{(d)}, X_2^{(d)})$ and $\tilde{V}^{(d)}$ denote the random variables having the long-run distribution of $X^{(d)}(t)$ and $\tilde{V}^{(d)}(t)$, respectively. Recall that in the discretisized version of the mobility formulation, we assumed the random variables $X^{(d)}(t)$ and $\tilde{V}^{(d)}(t)$ to take only discrete values, and in Lemma 3, provided the long-run proportion of times that a mobile stays in cell c_i, (i.e., $p_i^{(d)}$ in (20)), and possesses speed z_r (i.e., $\psi_r^{(d)}$ in (21)). Therefore, in order to derive the distributions of $X^{(d)}$ and $\tilde{V}^{(d)}$, we need to focus on the limiting behavior of the discrete distributions given by Lemma 3 as discretization parameters n and m approaches infinity.

As an illustration of the methodology that is going to be applied during this transition, lets concentrate on the simple mobility formulation whose discretisized version is depicted in Fig. 3. Recall that, in that simple model $V = v$ (i.e., deterministic) and the other mobility characterization parameters can be arbitrary. Now for the discretisized case, let $P_n^{(d)}(\frac{a}{2})$ denote the long-run proportion of time mobile is located in the region $R(\frac{a}{2}) = [0, \frac{a}{2}] \times [0, \frac{a}{2}]$. Hence, if $d = 4$ and $n = 4$, we have

$$P_4^{(4)}(\tfrac{a}{2}) = p_0^{(4)} \tag{28}$$

where $p_0^{(4)}$ is defined by (26). Notice that in this formulation the discretization parameter m is skipped because since $V = v$, $m = 1$.

Next, the important question is what will be the limiting form of $P_n^{(4)}(\frac{a}{2})$ in (28) as $n \to \infty$. Hence, if we assume $n = 16$, then discretisized region given in Fig. 3 will be transformed to form given in Fig. 4. By applying Lemma 3 we have

$$P_{16}^{(4)}(\tfrac{a}{2}) = \frac{\sum\limits_{c_i \in \tilde{R}(\frac{a}{2})} \varphi_i \, (1 - \tau_{i|i}) E[T_{p_i}] + \sum\limits_{c_i \in \tilde{R}(\frac{a}{2})} k_{i,1}^{(4)}}{N_{16,1}^{(4)}}, \tag{29}$$

where $\tilde{R}(\frac{a}{2}) = \{c_0, c_1, c_4, c_5\}$, that is, the set of discrete cells located on the region $R(\frac{a}{2})$.

Now based on the interpretation of $k_{i,r}^{(d)}$ in (22), the term $\sum_{c_i \in \tilde{R}(\frac{a}{2})} k_{i,1}^{(4)}$ corresponds to the average time spent over $R(\frac{a}{2})$ while moving between randomly picked two cells. Notice that both of those cells or one of them can be also belong to $\tilde{R}(\frac{a}{2})$. Hence we reach to the following:

$$\sum_{c_i \in \tilde{R}(\frac{a}{2})} k_{i,1}^{(4)} = \sum_{c_j \in \tilde{R}} \sum_{c_{i'} \in \tilde{R}} \varphi_{i'} \, \tau_{j|i'} \, P_{(\frac{a}{2})}(i', j) \, \frac{1}{v} \, J_{(\frac{a}{2})}(i', j) \, \Delta c^{(d)} \tag{30}$$

where $P_{(\frac{a}{2})}(i', j)$ denotes the probability passing over the region $R(\frac{a}{2})$ while moving from $c_{i'}$ to c_j, and $J_{(\frac{a}{2})}(i', j)$ represents the number of discrete jumps over $R(\frac{a}{2})$ while moving. Notice that the term $J_{(\frac{a}{2})}(i', j) \, \Delta c^{(d)}$ represents the total distance traveled over $R(\frac{a}{2})$, which is required to calculate the average time spent.

Therefore, in order to obtain the limiting form of $P_n^{(4)}(\frac{a}{2})$ as $n \to \infty$, we need to derive the limiting expression of the double summation given in (30) which requires a proper formulation of $P_{(\frac{a}{2})}(i', j)$ and $J_{(\frac{a}{2})}(i', j)$.

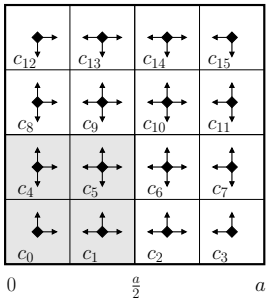

Fig. 4. Increasing the discretization scale of Fig. 3 ($n = 16$, $d = 4$).

Thus, we now focus on the formalization of the observations we mentioned above. In order to keep our formulation as simple as possible, we concentrate on deriving the long-run distributions of the continuous-4 (i.e., $d = 4$) and continuous-6 (i.e., $d = 6$) mobility formulations over square and hexagonal mobility terrains of side length a, respectively. Denote these terrains with the generic notation $R^{(d)}(a)$, where d is substituted by 4 if it is a square, else by 6 (i.e., hexagon). Also, to describe long-run location distribution consistently with d and the shape of mobility terrain (i.e., $R^{(d)}(a)$), we focus on defining the probability mass function (pmf) of $X^{(d)}$ over a square subregion in $R^{(4)}(a)$, and a hexagonal subregion in $R^{(6)}(a)$. Let $R^{(d)}(x, b)$ denote these subregions, which is a square if $d = 4$, and a hexagon if $d = 6$, with center $x \in R^{(d)}(a)$ and side length b such that $R^{(d)}(x, b) \subseteq R^{(d)}(a)$. In Fig. 5 and Fig. 6, we provided illustrations of $R^{(d)}(a)$ and $R^{(d)}(x, b)$, $d = 4, 6$. Notice that, $R^{(6)}(x, b)$ represents the subregion surrounded by the vertices $(x_1 \pm b, x_2)$, $(x_1 \pm \frac{b}{2}, x_2 \pm \frac{b\sqrt{3}}{2})$, where $x = (x_1, x_2)$. We also denote by $\mathcal{S}^{(d)}(a, b)$ the set of all nonintersecting $R^{(d)}(x, b) \subseteq R^{(d)}(a)$.

In addition to the these notations, let $L^{(d)}(p, x_s, x_d, x, b, a)$ denote the length of the total distance traveled over the subregion $R^{(d)}(x, b)$ for a movement epoch that occurs between the points x_s and x_d, and passes through $R^{(d)}(x, b)$ with probability p, which can be equal to 1, $\frac{1}{2}$, or 0 for the continuous-d mobility formulation. In Fig. 5 and Fig. 6 we depicted $L^{(d)}(p, x_s, x_d, x, b, a)$ for example movement epochs. Finally, we define

$$S^{(d)}(p, x_d, x, b) = \{x_s | x_s \in R^{(d)}(a), L^{(d)}(p, x_s, x_d, x, b, a) \neq 0\} \tag{31}$$

Based on the notations given in the preceding three paragraphs, we are now ready to state the main theorem of this section.

Theorem 1: For the mobile terminal, whose mobility pattern is characterized by the continuous-d mobility formulation over the mobility terrain $R^{(d)}(a)$, $d = 4, 6$, let $F_{X^{(d)}}(x, a, b)$ denote pmf of $X^{(d)}$ over the subregion $R^{(d)}(x, b) \subseteq R^{(d)}(a)$. Also, let $f_{\tilde{V}^{(d)}}$ denote the pdf of $\tilde{V}^{(d)}$.

If the pdf $f_{X_s}(x_d)$ can be uniquely determined from the integral equation (9), and $E[T_p | X_s = x_s] < \infty$, $\forall \, x_s \in R^{(d)}(a)$, and $f_{V|X_s, X_d} > 0$, $\forall \, v \in [v_{min}, v_{max}]$, and $\forall \, x_s, x_d \in$

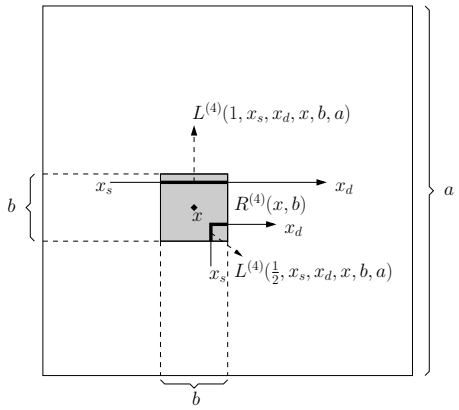

Fig. 5. Illustrations of $R^{(4)}(a)$, $R^{(4)}(x, b)$, and $L^{(4)}(p, x_s, x_d, x, b, a)$.

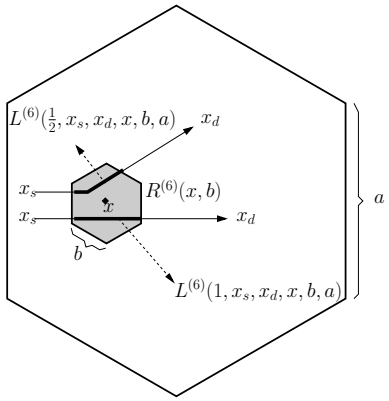

Fig. 6. Illustrations of $R^{(6)}(a)$, $R^{(6)}(x, b)$, and $L^{(6)}(p, x_s, x_d, x, b, a)$.

$R^{(d)}(a)$, then

$$F_{X^{(d)}}(x, a, b) = \frac{E[T_p|X_s \in R^{(d)}(x,b)] \Pr\{X_s \in R^{(d)}(x,b)\} + \int_{v_{min}}^{v_{max}} K^{(d)}(x,v,b,a)\, dv}{E[T_p|X_s \in R^{(d)}(a)] + \hat{D}^{(d)}}, \quad (32)$$

and

$$f_{\tilde{V}^{(d)}}(\tilde{v}) = \begin{cases} \frac{E[T_p|X_s \in R^{(d)}(a)]\delta(\tilde{v})}{E[T_p|X_s \in R^{(d)}(a)] + \hat{D}^{(d)}}, & \tilde{v} = 0 \\ \frac{\sum_{R^{(d)}(x,b) \in \mathcal{S}^{(d)}(a,b)} K^{(d)}(x,\tilde{v},b,a)}{E[T_p|X_s \in R^{(d)}(a)] + \hat{D}^{(d)}}, & \tilde{v} \in [v_{\min}, v_{\max}] \end{cases} \quad (33)$$

where

$$K^{(d)}(x, v, b, a) = \int_{x_d \in R^{(d)}(a)} dx_d \Big(\int_{x_s \in S^{(d)}(1,x_d,x,b)} dx_s\ k^{(d)}(1, x_s, x_d, x, v, b, a) + \frac{1}{2} \int_{x_s \in S^{(d)}(1/2,x_d,x,b)} dx_s\ k^{(d)}(1/2, x_s, x_d, x, v, b, a) \Big), \quad (34)$$

$$k^{(d)}(p, x_s, x_d, x, v, b, a) = f_{X_s}(x_s) f_{X_d|X_s}(x_d|x_s) \tfrac{1}{v} f_{V|X_s,X_d}(v|x_s, x_d) L^{(d)}(p, x_s, x_d, x, b, a), \quad (35)$$

and

$$\hat{D}^{(d)} = \sum_{R^{(d)}(x,b) \in \mathcal{S}^{(d)}(a,b)} \int_{v_{\min}}^{v_{\max}} dv\ K^{(d)}(x, v, b, a) \quad (36)$$

Proof: Refer to Appendix II. ■

We may note that the term $\int_{v_{min}}^{v_{max}} K^{(d)}(x,v,b,a)\, dv$, where $K^{(d)}(x, v, b, a)$ is given in (34), corresponds to the expected time spent over the region $R^{(d)}(x, b)$ while moving between the points X_s and X_d that are respectively drawn from the distributions f_{X_s} and $f_{X_d|X_s}$. Also, in order to formulate $L^{(d)}(p, x_s, x_d, x, b, a)$ and the region $S^{(d)}(p, x_d, x, b)$ explicitly we need to partition $R^{(d)}(a)$ with respect to $R^{(d)}(x, b)$. Clearly this will increase the complexity of the results presented by Theorem 1. However since we are aimed at using the distributions of the continuous-d case to reach some conclusions about the exact case, we decided to keep the presentation of the results given by Theorem 1 as simple as possible.

Now, in view of the result given by Claim 1 for $\hat{D}_n^{(d)}$ (25), if V (i.e., the speed for a movement epoch) is assumed to be independent from the distributions of X_s and X_d, then we get the following for $\hat{D}^{(d)}$ in (36).

$$\hat{D}^{(d)} = E[\frac{1}{V}]\bar{D}^{(d)} \quad (37)$$

where

$$\bar{D}^{(d)} = \int_{x_s \in R^{(d)}(a)} dx_s \int_{x_d \in R^{(d)}(a)} dx_d\, f_{X_s}(x_s) f_{X_d|X_s}(x_d|x_s)\, |x_s - x_d|^{(d)} \quad (38)$$

where $|x_s - x_d|^{(d)}$ represent the total distance traveled between the points $x_s = (x_{s_1}, x_{s_2})$ and $x_d = (x_{d_1}, x_{d_2})$ for the continuous-d mobility formulation. Clearly if $d = 4$, then

$$|x_s - x_d|^{(4)} = |x_{d_1} - x_{s_1}| + |x_{d_2} - x_{s_2}| \quad (39)$$

which is also know as the *Manhattan distance* [12]. Also, notice that $|x_s - x_d|^{(4)} > |x_s - x_d|^{(6)}$, $\forall x_s, x_d \in R$.

Finally, based on the definition of $\bar{D}^{(d)}$ in (38), the $E[\tilde{V}^{(d)}]$ will be given by the following even if the distribution of V is dependent on the distributions of X_s and X_d.

$$E[\tilde{V}^{(d)}] = \frac{\bar{D}^{(d)}}{E[T_p|X_s \in R^{(d)}(a)] + \hat{D}^{(d)}} \quad (40)$$

IV. Properties of the Continuous Mobility Formulation

In this section, we concentrate on the long-run properties of the continuous mobility formulation. In order to be as generic as possible, the mobility terrain R is assumed to be rectangular defined by $R = [0, a_1] \times [0, a_2]$. Denote $X(t)$ and $V(t)$, respectively, as the location and speed of a mobile terminal at time t. Because we are interested in the long-run distributions, let X and $\tilde{V}$ respectively denote the random variables having the long-run distribution of $X(t)$ and $\tilde{V}(t)$. Notice that the state spaces of X and $X^{(d)}$, and $\tilde{V}$ and $\tilde{V}^{(d)}$ are the same but since the continuous-d mobility formulation puts restriction on the movement directions, their distributions will be always different from each other.

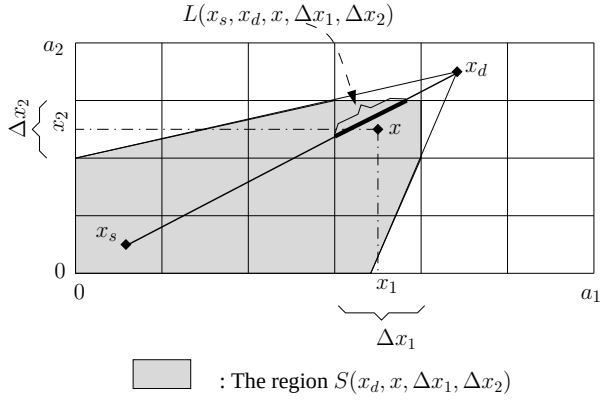

Fig. 7. Illustrations of $S(x_d, x, \Delta x_1, \Delta x_2)$ and $L(x_s, x_d, x, \Delta x_1, \Delta x_2)$ for the continuous mobility formulation.

Now as mentioned before, since d can be either equal to four or six, the results provided by Theorem 1 can not be extended formally to cover the exact case that allows mobile to move at any direction. However, we feel that since the formulation of $F_{X^{(d)}}(x, a, b)$ in (32) and $f_{\tilde{V}^{(d)}}(\tilde{v})$ in (33) are completely dependent the formulation of the region $S^{(d)}(p, x_d, x, b)$ in (31) that is composed of the points x_s where a movement starts with destination x_d and passes through the region $R^{(d)}(x, b)$ (see Fig. 5 and Fig. 6) with probability p, the formulation of the distributions for the continuous case should be also dependent on identifying the starting points where a movement epoch with a prespecified destination passes through a given subregion.

Therefore, analogous to the definition of $R^{(d)}(x, b)$ inside $R^{(d)}(a)$ (see Fig. 5 and Fig. 6), we define the following rectangular subregion for the continuous case:

$$R(x, \Delta x_1, \Delta x_2) = [x_1 - \tfrac{\Delta x_1}{2}, x_1 + \tfrac{\Delta x_1}{2}] \times [x_2 - \tfrac{\Delta x_2}{2}, x_2 + \tfrac{\Delta x_2}{2}] \quad (41)$$

where $x = (x_1, x_2)$, and Δx_1 and Δx_2 are selected such that $R(x, \Delta x_1, \Delta x_2) \subseteq R$. Also denote $\mathcal{S}(\Delta x_1, \Delta x_2)$ as the set of all nonintersecting $R(x, \Delta x_1, \Delta x_2) \subseteq R$.

Now since the direction of movement is not restricted, a movement epoch that starts from a point x_s with destination x_d passes through the region $R(x, \Delta x_1, \Delta x_2)$ with probability one or zero. Therefore, it is enough denote the distance traveled over $R(x, \Delta x_1, \Delta x_2)$ by $L(x_s, x_d, x, \Delta x_1, \Delta x_2)$. Hence, the correspondent of $S^{(d)}(p, x_d, x, b)$ in (31) is simply

$$S(x_d, x, \Delta x_1, \Delta x_2) = \{x_s | x_s \in R, L(x_s, x_d, x, \Delta x_1, \Delta x_2) \neq 0\} \quad (42)$$

In Fig. 7, we illustrated $S(x_d, x, \Delta x_1, \Delta x_2)$ and the line segment $L(x_s, x_d, x, \Delta x_1, \Delta x_2)$ for a destination point x_d outside the region $R(x, \Delta x_1, \Delta x_2)$.

In view of these discussions, we conjecture the following result, which is a plausible one but since the continuous-d mobility formulation is not defined for $d > 6$, it cannot be proven formally.

Conjecture 1: For the mobile terminal, whose mobility pattern is characterized by the triplet $< f_{X_d|X_s}, f_{V|X_s,X_d}, f_{T_p|X_d} >$, over the mobility terrain $R = [0, a_1] \times [0, a_2]$, let $F_X(x, \Delta x_1, \Delta x_2)$ denote pmf of X over the subregion $R(x, \Delta x_1, \Delta x_2)$ in (41). Also, let $f_{\tilde{V}}$ denote the pdf of $\tilde{V}$.

If the pdf $f_{X_s}(x_d)$ can be uniquely determined from the integral equation (9), and $E[T_p|X_s = x_s] < \infty$, $\forall x_s \in R$, and $f_{V|X_s,X_d} > 0$, $\forall v \in [v_{min}, v_{max}]$, and $\forall x_s, x_d \in R$, then

$$F_X(x, \Delta x_1, \Delta x_2) = \frac{E[T_p|X_s \in R(x, \Delta x_1, \Delta x_2)] \Pr\{X_s \in R(x, \Delta x_1, \Delta x_2)\}}{E[T_p|X_s \in R] + \hat{D}} + \frac{\int_{v_{min}}^{v_{max}} K(x, v, \Delta x_1, \Delta x_2)\, dv}{E[T_p|X_s \in R] + \hat{D}} \quad (43)$$

and

$$f_{\tilde{V}}(\tilde{v}) = \begin{cases} \frac{E[T_p|X_s \in R]\delta(\tilde{v})}{E[T_p|X_s \in R] + \hat{D}}, & \tilde{v} = 0 \\ \frac{\sum_{R(x,\Delta x_1,\Delta x_2) \in \mathcal{S}(\Delta x_1, \Delta x_2)} K(x, \tilde{v}, \Delta x_1, \Delta x_2)}{E[T_p|X_s \in R] + \hat{D}}, & \tilde{v} \in [v_{min}, v_{max}] \end{cases}, \quad (44)$$

where

$$K(x, v, \Delta x_1, \Delta x_2) = \int_{x_d \in R} dx_d \int_{x_s \in S(x_d, x, \Delta x_1, \Delta x_2)} dx_s\; k(x_s, x_d, x, v, \Delta x_1, \Delta x_2), \quad (45)$$

$$k(x_s, x_d, x, v, \Delta x_1, \Delta x_2) = f_{X_s}(x_s) f_{X_d|X_s}(x_d|x_s) \tfrac{1}{v} f_{V|X_s,X_d}(v|x_s, x_d) L(x_s, x_d, x, \Delta x_1, \Delta x_2), \quad (46)$$

and

$$\hat{D} = \sum_{R(x,\Delta x_1,\Delta x_2) \in \mathcal{S}(\Delta x_1, \Delta x_2)} \int_{v_{min}}^{v_{max}} dv\; K(x, v, \Delta x_1, \Delta x_2) \quad (47)$$

Now recall that for the continuous-d mobility formulation, if V is assumed to be independent from X_s and X_d, then $\hat{D}^{(d)} = E[\frac{1}{V}]\bar{D}^{(d)}$, where $\bar{D}^{(d)}$ is given by (38). Thus, we conjecture the following result:

Conjecture 2: If the distribution of V is assumed to be independent from X_s and X_d, then the $\hat{D}$ in (47) will be given by

$$\hat{D} = E[\frac{1}{V}]\bar{D} \quad (48)$$

where

$$\bar{D} = \int_{x_s \in R} dx_s \int_{x_d \in R} dx_d\, f_{X_s}(x_s) f_{X_d|X_s}(x_d|x_s)\, |x_s - x_d| \quad (49)$$

where $|x_s - x_d|$ denotes the euclidean distance between x_s and x_d.

In addition, from the formulation of $E[\tilde{V}^{(d)}]$ in (40), we reach to the following conclusion.

Conjecture 3: The expected value of $\tilde{V}$ with the pdf defined by (44) is

$$E[\tilde{V}] = \frac{\bar{D}}{E[T_p|X_s \in R] + \hat{D}} \quad (50)$$

Having defined $E[\tilde{V}]$ for the most generic case, we note that the analytical work presented in [7] also derives $f_{\tilde{V}}$ and

$E[\tilde{V}]$ for a class of mobility models where the speed of a movement epoch is selected independently from the distance that is going to be traveled for that epoch. In order to be able to compare our results with the ones given in that paper, we must consider the scenarios that the triplet $< f_{X_d}, f_V, f_{T_p} >$ is enough for mobility characterization, that is, distributions of X_d and T_p are independent from X_s, and V is independently selected from X_s and X_d. Hence, after simplifying $f_{\tilde{V}}$ in (44), and $E[\tilde{V}]$ in (50), we get

$$f_{\tilde{V}}(v) = \begin{cases} \frac{E[T_p]\delta(v)}{E[T_p]+E[\frac{1}{V}]\bar{D}}, & v{=}0 \\ \\ \frac{\frac{1}{v}f_V(v)\bar{D}}{E[T_p]+E[\frac{1}{V}]\bar{D}}, & v{\in}[v_{min},v_{max}] \end{cases}, \quad (51)$$

where $\delta(v)$ is defined as the direc delta function, and

$$E[\tilde{V}] = \frac{\bar{D}}{E[T_p] + E[\frac{1}{V}]\bar{D}}, \quad (52)$$

which are consistent with the ones given in [7].

A. Approximation to the pdf of long-run location distribution

Let f_X denote the pdf of X, that is, the random variable having the long-run distribution of $X(t)$. It then follows from the result given by Conjecture 1, and the definition given in [13] for the pdf of bivariate random variables that

$$f_X(x) = \lim_{\substack{\Delta x_1 \to 0 \\ \Delta x_2 \to 0}} \frac{F_X(x, \Delta x_1, \Delta x_2)}{\Delta x_1 \, \Delta x_2} \quad (53)$$

At this point, the important question is, given the triplet $< f_{X_d|X_s}, f_{V|X_s,X_d}, f_{T_p|X_d} >$, whether it is possible to find a closed form expression for the term $K(x, v, \Delta x_1, \Delta x_2)$ in (45) so that the above limit can be taken explicitly.

To answer this question, we first concentrate on a simple scenario where X_d is uniformly distributed over R for a given X_s, and V is characterized by f_V. Obviously for this case, $K(x, v, \Delta x_1, \Delta x_2)$ simplifies to

$$K(x, v, \Delta x_1, \Delta x_2) = \frac{f_V(v)}{v(a_1\, a_2)^2} \int_{x_d \in R} dx_d \int_{x_s \in S(x_d, x, \Delta x_1, \Delta x_2)} dx_s \; L(x_s, x_d, x, \Delta x_1, \Delta x_2) \quad (54)$$

Therefore, to be able to derive a closed form expression for $K(x, v, \Delta x_1, \Delta x_2)$, the integrand $L(x_s, x_d, x_i, \Delta x_1, \Delta x_2)$ must be expressible in terms of a function that can be analytically integrated over the given integration region.

Now from the definition of $L(x_s, x_d, x, \Delta x_1, \Delta x_2)$, and also from Fig. 7, observe that

$$L(x_s, x_d, x, \Delta x_1, \Delta x_2) = (g(x_s, x_d, x, \Delta x_1, \Delta x_2))^{1/2} \quad (55)$$

for a function $g(x_s, x_d, x, \Delta x_1, \Delta x_2)$ that is piecewisely continuous on $S(x_d, x, \Delta x_1, \Delta x_2)$ for given $x_d \in R$. Clearly, the analytical integration of $L(x_s, x_d, x, \Delta x_1, \Delta x_2)$ in (55) over the given 4-dimensional integration region (see (54)) is complicated. Hence, we conclude that obtaining a closed form expression for $K(x, v, \Delta x_1, \Delta x_2)$ even for the simplest of all possible mobility characterization parameters is nearly impossible.

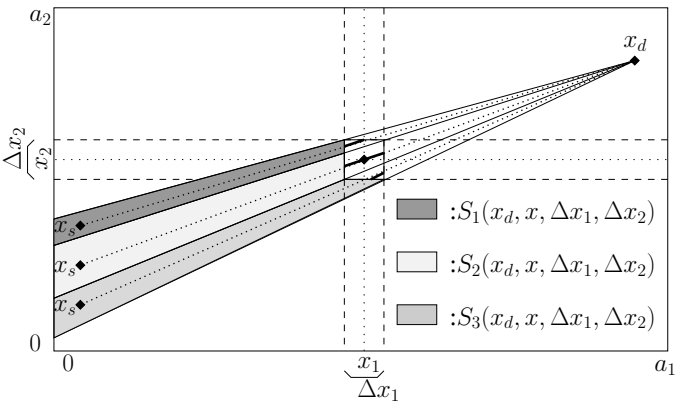

Fig. 8. Partitioning the region $S(x_d, x, \Delta x_1, \Delta x_2)$

However, if some exceptional choices of $x_s = (x_{s_1}, x_{s_2})$ and $x_d = (x_{d_1}, x_{d_2})$ are not taken into consideration, for example, suppose that $x_s, x_d \notin R(x, \Delta x_1, \Delta x_2)$, $|x_{d_1} - x_1| > \frac{\Delta x_1}{2}$, and $|x_{d_2} - x_2| > \frac{\Delta x_2}{2}$, then $L(x_s, x_d, x, \Delta x_1, \Delta x_2)$ will be expressible in terms of an easily integrable function for some mobility characterization choices.

To be more precise, on the rectangular mobility terrain $R = [0, a_1] \times [0, a_2]$ assume $x_{d_1} > x_1 + \frac{\Delta x_1}{2}$ and $x_{d_2} > x_2 + \frac{\Delta x_2}{2}$. Furthermore, let $\ell_R(x_1)$ denote the line segment joining the points x_d and $(x_1 + \frac{\Delta x_1}{2}, x_2 - \frac{\Delta x_2}{2})$, and assume $\ell_R(0) > 0$. In Fig. 8, we provided a visualization of these assumptions. Notice that this special case also implies $|x_{d_1} - x_{s_1}| > |x_{d_2} - x_{s_2}|$. In addition, consider the partitioning of the subregion $S(x_d, x, \Delta x_1, \Delta x_2)$ into three subregions as shown in Figure 8, and denote $L_r(x_s, x_d, x, \Delta x_1, \Delta x_2)$, $r = 1, 2, 3$, as the distance traveled over $R(x, \Delta x_1, \Delta x_2)$ when $x_s \in S_r(x_d, x, \Delta x_1, \Delta x_2)$. Next, formulating $L_r(x_s, x_d, x, \Delta x_1, \Delta x_2)$ explicitly we get

$$L_r(x_s, x_d, x, \Delta x_1, \Delta x_2) = \begin{cases} |x_d - x_s| \frac{\Delta x_1}{x_{d_1} - x_{s_1}}, & r{=}2 \\ \\ |x_d - x_s| \left(\frac{x_2 + c_r \frac{\Delta x_2}{2} - x_{s_2}}{x_{d_2} - x_{s_2}} - \frac{x_1 + c_r \frac{\Delta x_1}{2} - x_{s_1}}{x_{d_1} - x_{s_1}} \right), & r{=}1,3 \end{cases} \quad (56)$$

where $c_1 = 1$ and $c_3 = -1$.

Before we proceed further, it should be noted that, for the formulation that assumes $x_{d_1} > x_1 + \frac{\Delta x_1}{2}$ and $x_{d_2} > x_2 + \frac{\Delta x_2}{2}$, if we had concentrated on the case that only allows $|x_{d_2} - x_{s_2}| > |x_{d_1} - x_{s_1}|$, and had partitioned $S(x_d, x, \Delta x_1, \Delta x_2)$ in the same way as we did in Fig. 8, then the $L_r(x_s, x_d, x, \Delta x_1, \Delta x_2)$, $r = 1, 3$, would be also defined by (56). However, if $r = 2$, then

$$L_2(x_s, x_d, x, \Delta x_1, \Delta x_2) = |x_d - x_s| \frac{\Delta x_2}{x_{d_2} - x_{s_2}}, \quad (57)$$

which is expected intuitively.

Now returning back to case that is constructed according to the assumption $|x_{d_1} - x_{s_1}| > |x_{d_2} - x_{s_2}|$, it is clear that $L_2(x_s, x_d, x, \Delta x_1, \Delta x_2) > L_r(x_s, x_d, x, \Delta x_1, \Delta x_2)$, $r = 1, 3$ (also observe it from Fig. 8). Hence, concentrating on $L_2(x_s, x_d, x, \Delta x_1, \Delta x_2)$ observe the following:

$$L_2(x_s, x_d, x, \Delta x_1, \Delta x_2) = \Delta x_1 \sqrt{1 + \frac{(x_{d_2} - x_{s_2})^2}{(x_{d_1} - x_{s_1})^2}}, \quad (58)$$

Obviously as the difference between $|x_{d_1}-x_{s_1}|$ and $|x_{d_2}-x_{s_2}|$ increases, the term $\frac{(x_{d_2}-x_{s_2})^2}{(x_{d_1}-x_{s_1})^2}$ converges to zero. Hence, we can state the following:

$$L_2(x_s, x_d, x, \Delta x_1, \Delta x_2) \approx \Delta x_1 \tag{59}$$

Finally, since $L_2(x_s, x_d, x, \Delta x_1, \Delta x_2)$ is always more dominant than $L_r(x_s, x_d, x, \Delta x_1, \Delta x_2)$, $r = 1, 3$, we conclude the following approximation.

$$L(x_s, x_d, x, \Delta x_1, \Delta x_2) \approx \begin{cases} \Delta x_1, & |x_{d_1}-x_{s_1}| > |x_{d_2}-x_{s_2}| \\ \Delta x_2, & |x_{d_1}-x_{s_1}| < |x_{d_2}-x_{s_2}| \end{cases} \tag{60}$$

V. Example Scenarios

Example 1: The random waypoint model proposed in [4], which is commonly used to model node movement by the performance analysis studies for wireless ad hoc networks, can be considered as the simplest nontrivial case for the mobility characterizations that can be analyzed according to the triplet $< f_{X_d|X_s}, f_{V|X_s,X_d}, f_{T_p|X_d} >$. For this model, the distributions of X_d and V are assumed to be uniform in the regions R and $[v_{min}, v_{max}]$, respectively. Moreover, the distribution of T_p is considered to be the same at all destinations. Therefore, for the rectangular mobility terrain $R = [0, a_1] \times [0, a_2]$, we simply have

$$f_{X_s}(x_d) = \begin{cases} \frac{1}{a_1\, a_2}, & \text{if } x_d \in [0, a_1] \times [0, a_2] \\ 0, & \text{otherwise} \end{cases} \tag{61}$$

Hence, form Conjectures 1 and 2 we reach the following end result for the pmf of X over $R(x, \Delta x_1, \Delta x_2)$ in (41):

$$F_X(x, \Delta x_1, \Delta x_2) = \frac{\frac{E[T_p]\Delta x_1\, \Delta x_2}{a_1\, a_2} + E[\frac{1}{V}] K_X(x, \Delta x_1, \Delta x_2)}{E[T_p] + E[\frac{1}{V}]\bar{D}} \tag{62}$$

where

$$K_X(x, \Delta x_1, \Delta x_2) = \int_{x_d \in R} dx_d \int_{x_s \in S(x_d, x, \Delta x_1, \Delta x_2)} dx_s \, \frac{1}{(a_1 a_2)^2} L(x_s, x_d, x, \Delta x_1, \Delta x_2) \tag{63}$$

where $E[\frac{1}{V}] = \frac{\ln(\frac{v_{max}}{v_{min}})}{(v_{max}-v_{min})}$, and $\bar{D}$ is given by (49). In addition, $f_{\tilde{V}}$ and $E[\tilde{V}]$ can be derived respectively from the equations in (51), and (52).

In order to establish confidence in the correctness of the $F_X(x, \Delta x_1, \Delta x_2)$ we provided above by (62) for the random waypoint model, we will now focus on the task of evaluating $F_X(x, \Delta x_1, \Delta x_2)$ in (62) numerically for all $R(x, \Delta x_1, \Delta x_2) \in \mathcal{S}(\Delta x_1, \Delta x_2)$, and validating them using the results derived from the simulation of the random waypoint mobility model.

Hence, observe first that to generate $F_X(x, \Delta x_1, \Delta x_2)$ from (62) for a given $R(x, \Delta x_1, \Delta x_2)$, we need to evaluate $K_X(x, \Delta x_1, \Delta x_2)$ numerically in (63), which is defined by a 4-dimensional integral. Obviously, the accuracy of a result that can be derived from a numerical integration methodology is dependent on the *smoothness* of the integrand over the integration region [14]. Therefore, to increase the accuracy of our numerical experiments, we partition the region $S(x_d, x, \Delta x_1, \Delta x_2)$ into s_r subregions, where $s_r \geq 1$, so that the integrand $L(x_s, x_d, x, \Delta x_1, \Delta x_2)$ (see (63)) evaluated for a fixed x_d deviates less for all of the x_s that belongs to those subregions. In Fig. 9, we illustrated this partitioning methodology for a given x_d. Next, to evaluate the 4-dimensional integrals for each of these subregions, we first transformed them to an integral over a hypercube [14]. Then, each of the resulting integrals are evaluated by repeated one-dimensional integrations according to the Gauss' Formula [15]. Clearly, this is not "economical", however, it is required in order to provide an evidence for our conjecture. The program implementing this methodology is designed in a generic form in order to also capture different mobility characterization parameters, and it is available from authors.

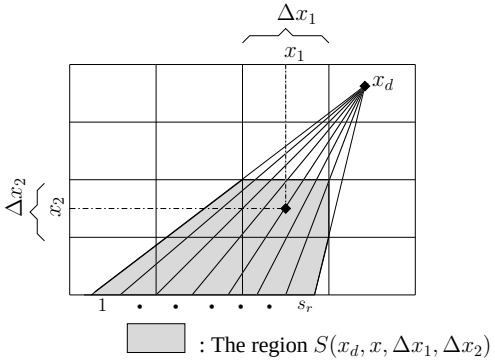

Fig. 9.Partitioning of $S(x_d, x, \Delta x_1, \Delta x_2)$ into s_r subregions for a given x_d.

To find $F_X(x, \Delta x_1, \Delta x_2)$ from simulation, a simple simulation model is developed consisting of a single node moving according to the random waypoint mobility profile. In this model, during each simulation run, the node travels for n_e number of movement epochs. For each movement epoch, the time spent at each $R(x, \Delta x_1, \Delta x_2) \in \mathcal{S}(\Delta x_1, \Delta x_2)$, while passing through it or pausing at it, is exactly calculated, and added to the total time spent at the subregion $R(x, \Delta x_1, \Delta x_2)$ for the whole simulation run. At the end of the run, $F_X(x, \Delta x_1, \Delta x_2)$ is derived by normalizing the total time spent at $R(x, \Delta x_1, \Delta x_2)$ to the total run time of the experiment. n_r independent replications of this experiment is run, and the final $F_X(x, \Delta x_1, \Delta x_2)$ is obtained by averaging the results of these runs. Also, at the beginning of each replication, the initial location, and speed and pause time distributions of the node is determined according to the methodology explained in [6] for the efficient and reliable simulation of random waypoint mobility model.

Now to be able to represent a comparison of the results obtained form (62), and from the simulation model we described above, consider the region $[b_1^{(1)}, b_2^{(1)}] \times [b_1^{(2)}, b_2^{(2)}] \subseteq R$ where $b_i^{(1)}, i = 1, 2$, and $b_j^{(2)}, j = 1, 2$, are multipliers of Δx_1 and Δx_2, respectively. Notice that if $P_X(b^{(1)}, b^{(2)})$ denotes the probability of the mobile terminal to be located over the region $[b_1^{(1)}, b_2^{(1)}] \times [b_1^{(2)}, b_2^{(2)}]$ at the long-run, then $P_X(b^{(1)}, b^{(2)})$ can be easily derived by accumulating all of the $F_X(x, \Delta x_1, \Delta x_2)$ such that $R(x, \Delta x_1, \Delta x_2) \subset [b_1^{(1)}, b_2^{(1)}] \times [b_1^{(2)}, b_2^{(2)}]$. Hence, let $P_X^{(C)}(b^{(1)}, b^{(2)})$ and $P_X^{(S)}(b^{(1)}, b^{(2)})$ respectively denote the correspondent of $P_X(b^{(1)}, b^{(2)})$ obtained from (62) (i.e., Conjecture 1) and from the simulation model. Based on these notations, we define the following metric to asses the

Percentage of Error: $E_X^{(S,C)}(b^{(1)},b^{(2)})\times 100$								
a_2	1.237	0.425	0.352	0.4	0.355	0.323	0.345	1.231
$\frac{a_2}{6}$	0.563	0.212	0.223	0.194	0.216	0.259	0.241	0.494
$\frac{a_2}{6}$	0.491	0.254	0.133	0.143	0.167	0.246	0.256	0.41
$\frac{a_2}{6}$	0.688	0.183	0.127	0.171	0.25	0.2	0.215	0.501
$\frac{a_2}{6}$	0.632	0.226	0.226	0.221	0.259	0.205	0.159	0.709
$\frac{a_2}{6}$	1.04	0.316	0.385	0.346	0.353	0.291	0.468	1.291
0	0	$\frac{a_1}{8}$	$\frac{2a_1}{8}$	$\frac{3a_1}{8}$	$\frac{4a_1}{8}$	$\frac{5a_1}{8}$	$\frac{6a_1}{8}$	$\frac{7a_1}{8}$ a_1

(a)

Percentage of Error: $E_X^{(C,A)}(b^{(1)},b^{(2)})\times 100$								
a_2	5.163	0.519	1.373	2.088	2.088	1.373	0.519	5.163
$\frac{a_2}{6}$	2.077	0.324	0.553	1.058	1.058	0.553	0.324	2.077
$\frac{a_2}{6}$	0.883	0.073	0.196	0.158	0.158	0.196	0.073	0.883
$\frac{a_2}{6}$	0.883	0.073	0.196	0.158	0.158	0.196	0.073	0.883
$\frac{a_2}{6}$	2.077	0.324	0.553	1.058	1.058	0.553	0.324	2.077
$\frac{a_2}{6}$	5.163	0.519	1.373	2.088	2.088	1.373	0.519	5.163
0	0	$\frac{a_1}{8}$	$\frac{2a_1}{8}$	$\frac{3a_1}{8}$	$\frac{4a_1}{8}$	$\frac{5a_1}{8}$	$\frac{6a_1}{8}$	$\frac{7a_1}{8}$ a_1

(b)

Fig. 10. $E_X^{(S,C)}(b^{(1)},b^{(2)})$ in (64) and $E_X^{(S,A)}(b^{(1)},b^{(2)})$ in (70) for Example 1 ($a_1=1200$, $a_2=900$, $b_1^{(1)}=i\,a_1/8,\ i=0,\ldots,7$, $b_2^{(1)}=b_1^{(1)}+a_1/8$, $b_1^{(2)}=j\,a_2/6,\ j=0,\ldots,5$, $b_2^{(2)}=b_1^{(2)}+a_2/6$, $v_{min}=1$ m/s, $v_{\rm min}=20$ m/s, $T_p=U[0,30]$ sec).

correctness of our conjecture for this mobility model.

$$E_X^{(S,C)}(b^{(1)},b^{(2)})=\frac{|P_X^{(S)}(b^{(1)},b^{(2)})-P_X^{(C)}(b^{(1)},b^{(2)})|}{P_X^{(S)}(b^{(1)},b^{(2)})}, \tag{64}$$

Finally, for our experiments, we considered a $[0,1200]$m $\times[0,900]$m mobility terrain, and set the parameters of mobility as follows: $v_{min}=1$m/s, $v_{min}=20$m/s, and T_p is uniform over the range $[0,30]$sec. Then, we chose $\Delta x_1=\Delta x_2=5$m, and set $n_e=10^7$, $n_r=100$ for the simulation experiment, and evaluated $E_X^{(S,C)}(b^{(1)},b^{(2)})$ for various choices of $b_i^{(1)}$ and $b_i^{(2)}, i=1,2$. The results are presented in Fig. 10.(a). Simulation results are acquired with a 95% confidence interval lower than 0.001. Since the percentage of error, (i.e., $E_X^{(S,C)}(b^{(1)},b^{(2)})\times 100$) is at most 1.29% we conclude that the application of the Conjecture 1 to random waypoint mobility model is correct.

Thus, using $F_X(x,\Delta x_1,\Delta x_2)$ in (62) we can obtain the pmf of $X=(X_1,X_2)$ over the subregion $R(x,\Delta x_1,\Delta x_2)$ numerically. With this knowledge at hand, we will now concentrate on finding $E[X_1]$, $E[X_2]$, and $Corr(X_1,X_2)$. Hence, we set $\Delta x_1=\frac{a_1}{n_1}$ and $\Delta x_2=\frac{a_2}{n_2}$ for some discretization parameters $n_1,n_2\in\mathbf{Z}^+$, and define the discrete bivariate random variable $X^*=(X_1^*,X_2^*)$ with the finite state space

$$\mathcal{S}^*=\left\{\tfrac{\Delta x_1}{2},\tfrac{3\Delta x_1}{2},\ldots,\tfrac{(2n_1-1)\Delta x_1}{2}\right\}\times\left\{\tfrac{\Delta x_2}{2},\tfrac{3\Delta x_2}{2},\ldots,\tfrac{(2n_2-1)\Delta x_2}{2}\right\} \tag{65}$$

to denote the subregion $R(x^*,\Delta x_1,\Delta x_2)$ in (41), where $x^*\in\mathcal{S}^*$, that the mobile is located at the long-run. Clearly, as $n_1\to\infty$ and $n_2\to\infty$, X^* converges to the continuous bivariate random variable X.

Evaluating the distribution of X^* from $F_X(x,\Delta x_1,\Delta x_2)$ in (62) we obtained $E[X_1^*]$, $E[X_2^*]$, and $Corr(X_1^*,X_2^*)$ numerically for several different parameter choices for the random waypoint mobility model. For all of the scenarios we considered, we set n_1 and n_2 sufficiently large enough to closely approximate $X=(X_1,X_2)$ with $X^*=(X_1^*,X_2^*)$, and observed the following:

$$E[X_1^*]=\frac{a_1}{2},\ \ E[X_2^*]=\frac{a_2}{2},\ \ Corr(X_1^*,X_2^*)=0 \tag{66}$$

The simulation studies presented in [16], [17] points out that the long-run location distribution of the random waypoint mobility model is more accumulated at the center of the mobility terrain. More importantly, it is symmetric with respect to center. Therefore, obtaining $E[X_1^*]$ and $E[X_2^*]$ as in (66) is expected. However, the result for $Corr(X_1^*,X_2^*)=0$ is not observed before. Obviously, it does not conclude that the distributions of X_1 and X_2 are independent.

It should also be noted that analytical work presented in [5] for the spatial node distribution generated by this mobility model concentrates on the case where $R=[0,a]\times[0,a]$, V is deterministic with parameter v, and $E[T_p]=0$, and formulates the long-run cumulative distribution function over a region with an area of δ^2. If we substitute $E[1/V]$ with $\frac{1}{v}$, and $E[T_p]=0$, and assume $\Delta x_1=\Delta x_2=\delta$, and $a_1=a_2$, the $F_X(x,\Delta x_1,\Delta x_2)$ we defined by (62) becomes consistent with the formulation of the cumulative distribution function given in [5].

We now focus on applying the approximation we defined by (60) for $L(x_s,x_d,x,\Delta x_1,\Delta x_2)$ to derive an approximation to $f_X(x)$ in (53) (i.e., the pdf of X). First, notice from the formulation of $K_X(x,\Delta x_1,\Delta x_2)$ in (63) that when this approximation is used, the integration of the integrand over the region $S(x_d,x,\Delta x_1,\Delta x_2)$, will be equal to Δx_1 or Δx_2 times the area of the region $S(x_d,x,\Delta x_1,\Delta x_2)$. Hence, by partitioning the boundaries of the 4-dimensional integration that formulates $K_X(x,\Delta x_1,\Delta x_2)$ according to the condition $|x_{d_1}-x_{s_1}|>|x_{d_2}-x_{s_2}|$ and its counterpart appropriately, we obtained a closed form expression for (63). Finally, evaluating the limit $\frac{F_X(x_i,\Delta x_1,\Delta x_2)}{\Delta x_1\,\Delta x_2}$ as $\Delta x_1\to 0$ and $\Delta x_2\to 0$, we reached the following approximation for f_X:

$$f_X(x)\approx\tilde{f}_X(x) \tag{67}$$

where

$$\tilde{f}_X(x)=\frac{E[T_p]\frac{1}{a_1\,a_2}+E[\frac{1}{V}]k(x)/\tilde{N}}{E[T_p]+E[\frac{1}{V}]\bar{D}} \tag{68}$$

where $k(x)$ is defined by the equation in (85) in Appendix I,

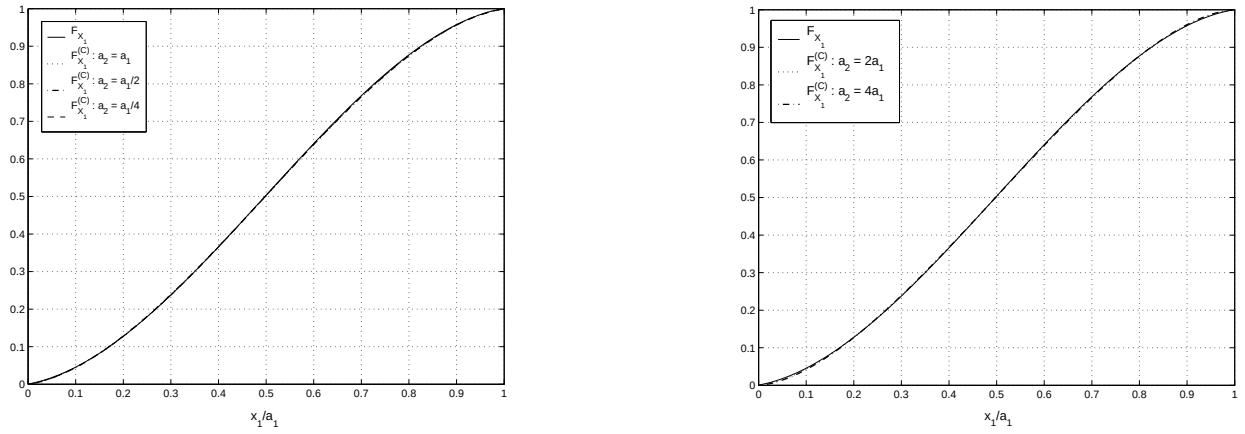

(a) (b)

Fig. 11. Comparison of F_{X_1} in (72) and $F_{X_1}^{(C)}$ in (73) for Example 2 ($a_1 = 1000$ m, $\Delta x_1 = \Delta x_2 = 5$m, $v_{min} = 1$ m/s, $v_{max} = 20$ m/s, $T_p = U[0, 30]$ sec).

and $\tilde{N}$ is the normalization term given by

$$\tilde{N} = \big(\int_{x \in R} k(x)\, dx \big) / \bar{D} \tag{69}$$

It should be noted that since the term $L(x_s, x_d, x, \Delta x_1, \Delta x_2)$ is either substituted by Δx_1 or Δx_2, the function $k(x)$ in (85) must be normalized in the region R so that $\tilde{f}_X(x)$ will be a probability density function.

In order to asses the validity of the approximation we presented above by (67), we define

$$E_X^{(C,A)}(b^{(1)}, b^{(2)}) = \frac{|P_X^{(C)}(b^{(1)}, b^{(2)}) - P_X^{(A)}(b^{(1)}, b^{(2)})|}{P_X^{(C)}(b^{(1)}, b^{(2)})}, \tag{70}$$

where $P_X^{(A)}(b^{(1)}, b^{(2)})$ is the integration of $\tilde{f}_X(x)$ in (68) over the region $[b_1^{(1)}, b_2^{(1)}] \times [b_1^{(2)}, b_2^{(2)}]$.

In Fig. 10.(b) we provided the $E_X^{(C,A)}(b^{(1)}, b^{(2)})$ for the same mobility parameter choices we considered in Fig. 10.(a). From the values of $E_X^{(C,A)}(b^{(1)}, b^{(2)})$ for different $[b_1^{(1)}, b_2^{(1)}] \times [b_1^{(2)}, b_2^{(2)}] \subseteq R$, we reached to the conclusion that the approximation we stated by (67) for the long-run spatial distribution of the random waypoint model over the given rectangular mobility terrain is quite accurate.

In addition, if one is interested in variant of random waypoint mobility model where mobiles may pause at different at different X_d, that is, $f_{T_p|X_d}$ needs to be employed in mobility characterization in stead of f_{T_p}, then the approximation given in (68) can be redefined as follows:

$$\tilde{f}_X(x) = \frac{E[T_p|X_s = x]\frac{1}{a_1\, a_2} + E[\frac{1}{V}]k(x)/\tilde{N}}{E[T_p|X_s \in R] + E[\frac{1}{V}]\bar{D}} \tag{71}$$

Finally, we note that in [5] authors also present a very accurate approximation for the pdf of X for the special case of the original random waypoint model where $R = [0, 1] \times [0, 1]$, and speed choice for all movement epochs is constant. In order to compare that approximation with the one given in this paper numerically for this special case (i.e., $R = [0, 1] \times [0, 1]$ and speed is constant), we evaluated cumulative long-run location distributions for several subregions over R according to both of them. We observed for various choices of $E[T_p]$ and V that the relative error between the results obtained from approximation and simulation is at most 2% for both of the approximation methods defined in [5] and in (67).

Example 2: According to the results that are proved in [1] for the one-dimensional version of the random waypoint mobility model, the probability distribution function of X_1 (i.e., the first component of $X = (X_1, X_2)$) over the mobility terrain $R = [0, a_1]$ is

$$F_{X_1}(x_1) = \frac{\frac{x_1}{a_1}E[T_p] + \frac{x_1^2(a_1 - 2x_1/3)}{a_1^2}E[\frac{1}{V}]}{E[T_p] + \frac{a_1}{3}E[\frac{1}{V}]} \tag{72}$$

In principle, if the application of Conjecture 1 to random waypoint model holds to be true, then the marginal distribution of X_1 derived from the joint probability distribution function $F_X(x, \Delta x_1, \Delta x_2)$, which is defined by (62) in Example 1 (i.e., the probability that $X = (X_1, X_2) \in R(x_i, \Delta x_1, \Delta x_2)$ at the long-run), and the probability distribution function F_{X_1} given above by (72) should match with each other. Thus, to provide an additional confidence to the $F_X(x, \Delta x_1, \Delta x_2)$ in (62) we conjectured for the random waypoint mobility model, we now concentrate on examining the correctness of this statement.

For this purpose, we first set $\Delta x_1 = \frac{a_1}{n_1}$ and $\Delta x_2 = \frac{a_2}{n_2}$ for some $n_1, n_2 \in \mathbf{Z}^+$. Hence, the marginal distribution function of X_1 can be derived from $F_X(x, \Delta x_1, \Delta x_2)$ (62) as follows:

$$\begin{aligned} F_{X_1}^{(C)}(x_1) &= \Pr\{X_1 \in [0, x_1] \times [0, a_2]\},\ x_1 = i\Delta x_1, i = 1, \ldots, n_1, \\ &= \sum_{i_1=1}^{\frac{x_1}{\Delta x_1}} \sum_{i_2=1}^{n_2} F_X(x_i, \Delta x_1, \Delta x_2) \end{aligned} \tag{73}$$

where $x = (x_1, x_2)$, that is, the center of the unit area $R(x, \Delta x_1, \Delta x_2)$ in (41).

In Fig. 11, we considered several proportions between a_1 and a_2 for the given mobility parameters, and provided a comparison of F_{X_1} in (72) and $F_{X_1}^{(C)}$ in (73) after evaluating $F_X(x, \Delta x_1, \Delta x_2)$ in (62) $\forall\ R(x_i, \Delta x_1, \Delta x_2) \in S(\Delta x_1, \Delta x_2)$ numerically according to the methodology we explained during the discussions for Example 1. As it can be observed from

Fig. 11, the two distribution functions perfectly matches with each other. Thus, we accomplished our goal in providing a second evidence for the application of Conjecture 1.

In addition, it is clear that an approximation to the marginal distribution of X_1 can be derived from the approximation defined by (68) for the joint probability density function of $X = (X_1, X_2)$. Therefore, we now define this approximation by

$$F_{X_1}^{(A)}(x_1) = \int_0^{x_1} du \int_0^{a_2} dv \tilde{f}_X(u, v) \tag{74}$$

where $\tilde{f}_X$ is given by (68).

Now from the comparisons of F_{X_1} in (72) and $F_{X_1}^{(A)}$ in (74) that are depicted graphically in Fig. 12 for the given mobility parameters, notice that the approximating results are very accurate for several proportions between a_1 and a_2. This observation is very important because it points out that the quality of approximation done by $F_{X_1}^{(A)}$ is insensitive to the frequency of the movement epochs that happen over the region $R = [0, a_1] \times [0, a_2]$ on the vertical and the horizontal directions.

Example 3: In Section IV we conjectured that if the distribution of V (i.e., the speed for a movement epoch) is independent from X_s and X_d, then the pdf of $\tilde{V}$ (i.e.,, $f_{\tilde{V}}$) and its expected value (i.e., $E[\tilde{V}]$) are given by equations (51) and (52), respectively. As we have mentioned before, those equations are consistent with the ones given in [7] for a class of mobility models where V selected independently from the distance that is going to be traveled (i.e., $|X_s - X_d|$).

Thus, for this example, we consider a variant of random waypoint mobility model which incorporates the ability to determine V according to $|X_s - X_d|$, and concentrate on the correctness on the distribution of $\tilde{V}$ we provided in Conjecture 1 for the most generic mobility characterization.

Now for the original random waypoint model, keeping the distributions of X_d and T_p the same as before, consider a truncated normal distribution [18] for V according to the pdf given by

$$f_{V|X_s,X_d}(v|x_s, x_d) = \frac{Z(\frac{v-\mu(x_s,x_d)}{\sigma})}{\sigma\big(\Phi(\frac{v_{max}-\mu(x_s,x_d)}{\sigma}) - \Phi(\frac{v_{min}-\mu(x_s,x_d)}{\sigma})\big)} \tag{75}$$

for $v_{min} \leq v \leq v_{max}$ where $\sigma > 0$, and

$$\mu(x_s, x_d) = v_{\min} + \frac{(v_{max} - v_{\min})}{a} |x_s - x_d| \tag{76}$$

Z and Φ are the probability density and cumulative distribution functions for the normal distribution [18].

Before proceeding further, observe from the formulation of $f_{V|X_s,X_d}$ that as $\sigma \to 0$ the possibility of determining V proportional to $|X_s - X_d|$ increases. Also, as $\sigma \to \infty$ we converge to the original case, that is, V is uniformly distributed in $[v_{min}, v_{max}]$.

Now formulating the $f_{\tilde{V}}$ according to the equation (44) provided in Conjecture 1, observe first that the integrand of $K(x, v, \Delta x_1, \Delta x_2)$ in (45) will be given by

$$k(x_s, x_d, x, v, \Delta x_1, \Delta x_2) = \frac{1}{v(a_1\, a_2)^2} f_{V|X_s,X_d}(v|x_s, x_d) L(x_s, x_d, x, \Delta x_1, \Delta x_2), \tag{77}$$

which implies that finding a closed form expression for $K(x, v, \Delta x_1, \Delta x_2)$ is very complicated even if the approximation defined by (60) for $L(x_s, x_d, x, \Delta x_1, \Delta x_2)$ is applied.

Therefore, to obtain the distribution of $\tilde{V}$ we use the numerical integration methodology we explained before in Example 1. Also, to test the accuracy of the numerical results obtained, we modified the simulation model we presented in Example 1 according the new mechanism to select V, and finally obtained the probability distribution function of $\tilde{V}$, (i.e., $F_{\tilde{V}}(v) = \int_{v_{min}}^{v} du f_{\tilde{V}}(u)$) both from the $f_{\tilde{V}}$ given in Conjecture 1 and the simulation model. In Fig. 13 we provided a comparison of these two results for different values of σ for the given mobility parameters. Simulation results are acquired with a 95% confidence interval lower than 0.003. Observe that, the two distributions perfectly matches with each other for all cases.

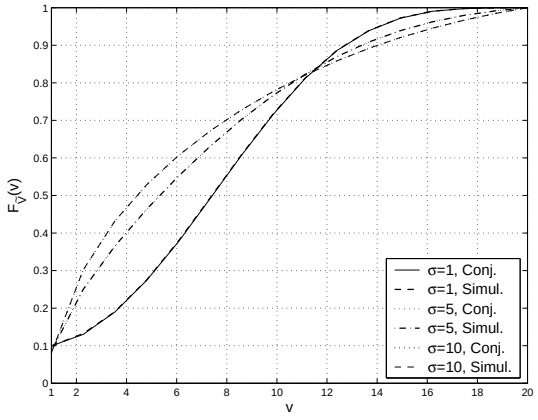

Fig. 13. Comparison of $F_{\tilde{V}}$ derived from Conjecture 1 and Simulation for Example 3 ($a_1 = 1200$ m, $a_2 = 900$ m, $\Delta x_1 = \Delta x_2 = 5$m, $v_{min} = 1$ m/s, $v_{max} = 20$ m/s, $T_p = U[0, 30]$ sec).

Having provided this confidence for the distribution of $\tilde{V}$ defined by Conjecture 1, we now focus on the effect of the choice of σ on the value of $E[\tilde{V}]$, which is also formulated by (50). In Table II we provided $E[\tilde{V}]$ for different choices of σ and $E[T_p]$. The other parameters are the same with the experiments performed for the results depicted in Fig. 13. First, observe that for a given $E[T_p]$, $E[\tilde{V}]$ increases as σ decreases. Also, for a given finite value of σ, the difference between the $E[\tilde{V}]$ obtained, and the $E[\tilde{V}]$ evaluated for the $\sigma \to \infty$ case increases as $E[T_p]$ increases. Both of these results are expected because as σ decreases, the possibility of moving long distances with artificially low speeds diminishes, and as a result, the expected value of the long-run speed increases.

Example 4: In the previous examples we assumed the distribution of X_d to be independent from X_s. To demonstrate the applicability of the generalized mobility framework we proposed to the scenarios where the choice of X_d is correlated with the starting point X_s, we will now concentrate on a variant of the Manhattan model introduced in [19] for the

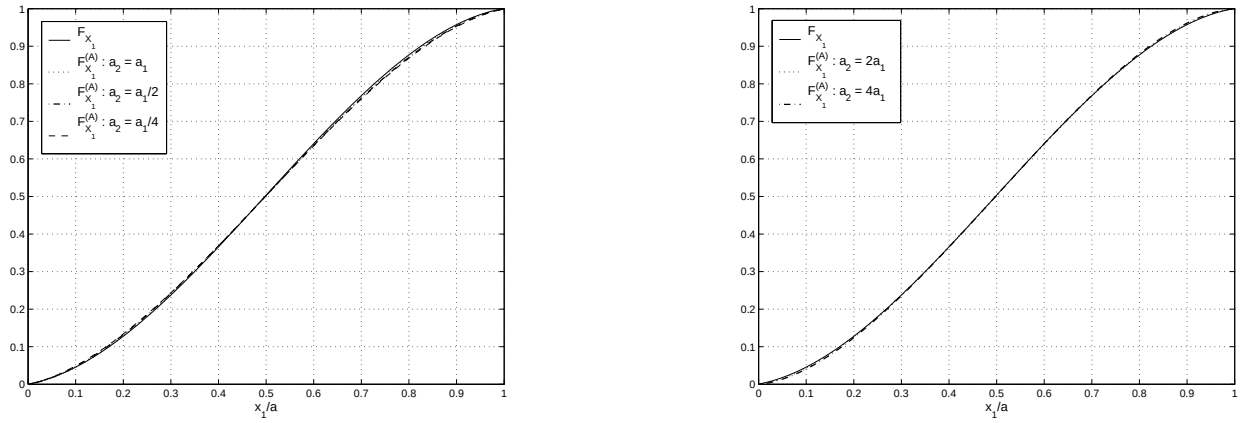

(a) (b)

Fig. 12. Comparison of F_{X_1} in (72) and $F_{X_1}^{(A)}$ in (74) for Example 2 ($a_1 = 1000$ m, $\Delta x_1 = \Delta x_2 = 5$m, $v_{min} = 1$ m/s, $v_{\max} = 20$ m/s, $T_p = U[0, 30]$ sec).

TABLE II
$E[\tilde{V}]$ FOR EXAMPLE 3

	$E[\tilde{V}]$ (m/s) ($v_{\min}$=1 m/s, v_{max}=20 m/s)			
$E[T_p]$ (sec)	$\sigma \to \infty$	$\sigma = 10$	$\sigma = 5$	$\sigma = 1$
0	6.342	6.517	6.867	8.106
15	5.408	5.985	6.279	7.299
30	4.713	5.535	5.785	6.638

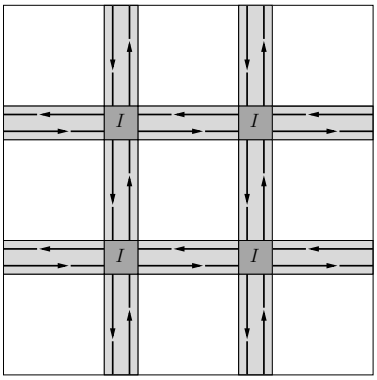

Fig. 14. Mobility terrain for the Manhattan mobility model.

simulation based performance analysis of wireless ad hoc networks.

In Manhattan model, mobile terminals are restricted to move towards horizontal and vertical directions on a mobility terrain that is composed of paths, which can be also call as "streets", forming a grid structure, as shown in Fig. 14. When a mobile enters to an intersection of streets it goes straight with probability p, which is set to $\frac{1}{2}$ in the model description. If it changes its direction, it selects either of the opposing directions with equal probabilities. Since this model is originally developed for simulation based studies, the speed of mobile terminals is characterized according to a sophisticated mechanism that imposes a correlation between the speed choices at the consecutive time slots of the discrete event simulation, and it can be dependent with the speed characteristics of other mobile terminals on the same street.

Now notice that in this model, the movement directions are limited by four, that is, $d = 4$, and they are given by γ_i, $i = 0, \ldots, d-1$ in (6). Hence, if the mobility profile formulated by Manhattan model can be characterized according to the triplet $< f_{X_d|X_s}, f_{V|X_s,X_d}, f_{T_p|X_d} >$, then the results presented in Theorem 1 for the continuous-4 mobility formulation can be directly applied for long-run analysis. Clearly since we assume the mobiles to move independently from each other, we cannot capture the speed formulation proposed by the Manhattan model. Hence, we can only concentrate on a variant of the original model where speed choices of terminals are independent from each other. We believe that even if this simplification is required, the other characteristic of the model is very important for the usability of our model because it corresponds to a scenario where mobiles are restricted to move on predefined paths.

For this purpose, and to be consistent with the notation used in Theorem 1, we assume that the two-dimensional mobility terrain R can be divided into equal size square subregions $R^{(4)}(x, b)$ of side length b with center x, as shown in Fig. 15. Also, each street is composed of many $R^{(4)}(x, b)$ forming a rectangle with side lengths b and a, where a is a multiple of b. In addition, intersections, which are represented by a single $R^{(4)}(x, b)$, either connect streets with each other, or streets to border of the mobility terrain.

Now to define the parameter $f_{X_d|X_s}$ (i.e., the pdf of X_d given X_s), assume that mobility epochs either start from a point over an intersection or a street. If epoch starts from a point belonging to an intersection, then with probability α, where $\alpha < 1$, it moves to a destination point that is distributed uniformly over one of the closest intersections, and with probability $1 - \alpha$ it selects a destination point uniformly over either of the connecting streets. On the other hand, if movement epoch starts from a point over a street, then with probability β, where $\beta < 1$, it moves to a destination over one of the connecting intersections, which is selected with equal probabilities, and with probability $1 - \beta$ the destination is selected at the same street. Again, in both cases, the destination point at the target subregion is uniformly distributed. In

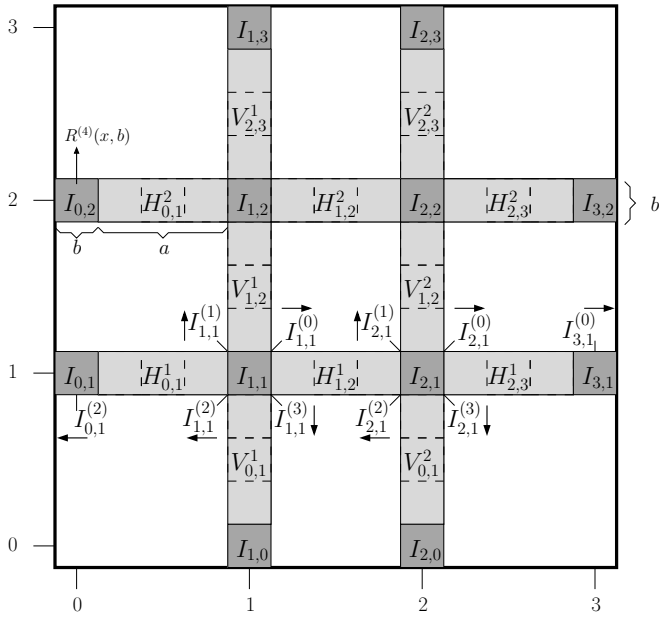

Fig. 15. Partitioning of the mobility terrain shown in Fig. 14.

addition, we assume that when a movement epochs ends(starts) at(from) an intersection it travels a total distance of $\frac{b}{2}$ inside that intersection. In other words, movement epochs occur between the centers of the intersections.

Clearly with this setting, mobiles may stop at streets. However, as $\alpha \to 1$, we converge to the scenario in which mobiles moves between intersections, which is also required by the original mobility model. We can not set $\alpha = 1$ because in that case locations over streets will never be selected as destination and the steady-state distribution for X_s will never exists. Also notice that by choosing $f_{T_p|X_d}$ (i.e., the pdf of pause time at the destination) appropriately, we can force the mobiles to not to stop at the intersections.

Now according to the Manhattan model when the mobile enters to the intersection, it either goes straight or turns. In order to model this, we need to have a mechanism that controls the direction of mobile terminals at consecutive movement epochs, which is not incorporated by the generalized mobility model we proposed. In our mobility framework, the destination point of the current movement epoch is dependent to the destination of the previous one, which becomes the starting point of the current, but not to its direction. However, if we separate the terminals entering an intersection according to the direction that they are coming trough, then we will have the opportunity to bring direction control into the mobility formulation.

More formally, consider the notations depicted in Fig. 15 for the identification of streets and intersections. When a mobile enters to an intersection, it takes a phase corresponding to the direction that it is coming trough. In Fig. 15 we provided a visualization of these phases for the intersections $I_{0,1}$, $I_{1,1}$, $I_{2,1}$, and $I_{3,1}$. Hence, $X_s \in I^{(\imath)}_{i,j}$ corresponds to the case where the mobile terminal enters to $I_{i,j}$ trough the direction $\gamma_\imath$. Since $I^{(\imath)}_{i,j}$ keeps the memory of previous direction, we can immediately model a scenario where mobile keeps the same direction with higher probability.

Thus, $f_{X_d|X_s}$ must be defined separately for all X_s belonging to intersections and streets. Concentrating on the special case $X_s \in I^{(0)}_{1,1}$, the stochastic density kernel $f_{X_d|X_s}$ will be defined as follows:

$$f_{X_d|X_s}(x_d|x_s) = \begin{cases} \frac{p\,\alpha}{b^2}, & X_s \in I^{(0)}_{1,1},\ X_d \in I^{(0)}_{2,1} \\ \frac{p\,(1-\alpha)}{a\,b}, & X_s \in I^{(0)}_{1,1},\ X_d \in H^1_{1,2} \\ \frac{(1-p)\,\alpha}{2\,b^2}, & X_s \in I^{(0)}_{1,1},\ X_d \in I^{(1)}_{1,2} \\ \frac{(1-p)\,(1-\alpha)}{2\,a\,b}, & X_s \in I^{(0)}_{1,1},\ X_d \in V^1_{1,2} \\ \frac{(1-p)\,\alpha}{2\,b^2}, & X_s \in I^{(0)}_{1,1},\ X_d \in I^{(3)}_{1,0} \\ \frac{(1-p)\,(1-\alpha)}{2\,a\,b}, & X_s \in I^{(0)}_{1,1},\ X_d \in V^1_{0,1} \end{cases}, \quad (78)$$

Clearly if the intersection is located near the border, then mobile is supposed to reflect back, and the kernel must be defined in a different way. For example, if $X_s \in I^{(2)}_{0,1}$, then we have

$$f_{X_d|X_s}(x_d|x_s) = \begin{cases} \frac{\alpha}{b^2}, & X_s \in I^{(2)}_{0,1},\ X_d \in I^{(0)}_{1,1} \\ \frac{1-\alpha}{a\,b}, & X_s \in I^{(2)}_{0,1},\ X_d \in H^1_{0,1} \end{cases}, \quad (79)$$

Finally, concentrating on $X_s \in H^1_{0,1}$, we have

$$f_{X_d|X_s}(x_d|x_s) = \begin{cases} \frac{\beta}{2\,b^2}, & X_s \in H^1_{0,1},\ X_d \in I^{(2)}_{0,1} \\ \frac{\beta}{2\,b^2}, & X_s \in H^1_{0,1},\ X_d \in I^{(0)}_{1,1} \\ \frac{1-\beta}{a\,b}, & X_s \in H^1_{0,1},\ X_d \in H^1_{0,1} \end{cases}, \quad (80)$$

For the rest of the cases, the kernel $f_{X_d|X_s}$ can be defined in a straightforward manner according to the conditions we considered in (78), (79), and (80).

As we have mentioned before, we cannot exactly capture the mobility formulation proposed by the original model. We have to assume that the speed characteristics of mobiles are independent from each other. In addition, as it is mentioned in Example 3, if the distribution of V is assumed to be dependent to the locations of X_s and X_d, then finding a closed from solution for the long-run location distribution is nearly impossible. Hence, we assume that the distribution of V is not correlated with the distributions of X_s and X_d. This is an reasonable assumption because since we are interested in the scenario where a movement epochs starts from a point on a intersection and without stopping at the streets ends up at one of the closest intersection (i.e., as $\alpha \to 1$), the distribution of speed can be immediately selected proportional to the length of a street, or according to the speed limit on streets.

Having defined the parameters of the mobility characterization, the next step is to derive the steady state distribution of X_s, that is to derive $f_{X_s}(x_d)$ from the integral equation in (9). For this purpose, let S_{d_k} denote the subregion (that is, street or intersection) that the X_d (i.e., destination point) of the kth movement epoch belongs to. Hence, the DTMC $\{S_{d_k}, k \in \mathbf{N}\}$ with states corresponding to the subregions $I^{(\imath)}_{i,j}$, $H^k_{i,j}$, and $V^k_{i,j}$ shown in Fig.15, and the transition probability matrix A that is constructed according to the formulation of $f_{X_d|X_s}$ can be used to govern the decisions of X_d at the embedded points in time when a new epoch starts. For instance, according to

(78) $\Pr\{S_{d_{k+1}} = I^{(0)}_{2,1} | S_{d_k} = I^{(0)}_{1,1}\} = p\,\alpha$ and $\Pr\{S_{d_{k+1}} = I^{(1)}_{1,2} | S_{d_k} = I^{(0)}_{1,1}\} = (1-p)\,\alpha/2$.

Thus, since we assume the destinations points to be uniformly distributed over an intersection or a street once that subregion is selected as destination, a steady-state distribution for X_s exists only if the DTMC $\{S_{d_k}, k \in \mathbf{N}\}$ satisfies the conditions of ergodicity. Therefore, α and β can not be equal to 1, which is already required in the formulation of $f_{X_d|X_s}$.

Now, let π denote the steady-state distribution of the DTMC $\{S_{d_k}, k \in \mathbf{N}\}$. After some algebraic manipulations we found out that

$$\pi_{I^{(\imath)}_{i,j}} = \tfrac{1}{C},\ \pi_{H^k_{i,j}} = \pi_{V^k_{i,j}} = \tfrac{2(1-\alpha)/\beta}{C}$$

where $C = 24(1 + (1-\alpha)/\beta)$. Since the $\{S_{d_k}, k \in \mathbf{N}\}$ determines the subregion X_s is located, it can be easily shown that the steady-state distribution of X_s has the following pdf:

$$f_{X_s}(x_d) = \begin{cases} \frac{1}{C\,b^2}, & {\scriptstyle x_d \in I^{(\imath)}_{i,j}} \\ \frac{2(1-\alpha)/\beta}{C\,a\,b}, & {\scriptstyle x_d \in H^k_{i,j},\, x_d \in V^k_{i,j}} \end{cases}, \qquad (81)$$

Next, for the case $\alpha \to 1$ (i.e., mobiles only stop at the intersection), let R_s denote subregion which represents the streets or the intersections, and denote P_{R_s} as the long-run proportion of time mobile terminals located at the at subregion R_s. Now, P_{R_s} can be derived as follows.

Since we have assumed the distribution of V to be independent from X_s and X_d, applying Theorem 1 we get the following form for P_{R_s}:

$$P_{S_r} = \frac{E[T_p | X_s \in R_s]\Pr\{X_s \in R_s\} + E[\frac{1}{V}] K_{R_s}}{E[T_p | X_s \in R] + E[\frac{1}{V}]\bar{D}^{(d)}} \qquad (82)$$

Now focusing on the term $\Pr\{X_s \in R_s\}$, assume that $R_s = I_{2,1}$. Since $I_{2,1}$ is composed of $I^{(\imath)}_{2,1}$ for $\imath = 0, \ldots, d-1$, $\Pr\{X_s \in I_{2,1}\} = 4\,b^2\,\frac{1}{C\,b^2} = \frac{1}{6}$. Clearly, if R_s was representing an intersection on the border, then it will be composed of a single $I^{(\imath)}_{i,j}$ for some $\imath \in \{0, \ldots, d-1\}$. Hence we can state the following:

$$\Pr\{X_s \in R_s\} = \begin{cases} \frac{1}{6}, & R_s = I_{i,j},\ \text{and } I_{i,j} \text{ is not on the border} \\ \frac{1}{24}, & R_s = I_{i,j},\ \text{and } I_{i,j} \text{ is on the border} \\ 0, & \text{otherwise} \end{cases} \qquad (83)$$

It should be that $\Pr\{X_s \in R_s\} = 0$ when R_s represents streets because as $\alpha \to 1$ the probability of selecting locations on streets as target diminishes.

In order to obtain the expression for K_{R_s}, we need to identify all of the movement epochs that pass trough subregion R_s including the ones starting and ending at R_s. Similar to what we did above assume $R_s = I_{2,1}$. The epochs that start from $I^{(0)}_{1,1}$ and $I^{(3)}_{2,2}$ will end up at $I_{2,1}$ with probability p, and the ones that originate from $I^{(1)}_{2,0}$ and $I^{(2)}_{3,1}$ will will target $I_{2,1}$ with probability 1. Also, the ones that start from $I^{(1)}_{1,1}$, $I^{(3)}_{1,1}$, $I^{(0)}_{2,2}$, and $I^{(2)}_{2,2}$, will move to $I_{2,1}$ with probability $\frac{(1-p)}{2}$. In addition, the epochs that originate from $I_{2,1}$ should be also taken into account. Hence, recalling that the distance traveled over an intersection is assumed to be equal to $\frac{b}{2}$, we get

$$K_{I_{2,1}} = 2\left(\tfrac{p\,b^2}{C\,b^2}\,\tfrac{b}{2} + 2\,\tfrac{(1-p)\,b^2}{2\,C\,b^2}\,\tfrac{b}{2} + 2\,\tfrac{b^2}{C\,b^2}\,\tfrac{b}{2}\right) + 4\,\tfrac{b^2}{C\,b^2}\,\tfrac{b}{2} = \tfrac{b}{6}$$

Base on this reasoning, we can state the following:

$$K_{R_s} = \begin{cases} \frac{b}{6}, & R_s = I_{i,j},\ \text{and } I_{i,j} \text{ is not on the border} \\ \frac{b}{24}, & R_s = I_{i,j},\ \text{and } I_{i,j} \text{ is on the border} \\ \frac{a}{12}, & R_s = H^k_{i,j} \text{ or } R_s = V^k_{i,j} \end{cases}, \qquad (84)$$

In addition, since movement epochs occur between intersections that can be joined by a single street, $\bar{D}^{(d)} = (a+b)$, which can be double checked by summing up K_{R_s} given above for all different R_s.

VI. Summary

This paper concentrates on the analysis of a generalized random mobility modeling approach for wireless ad hoc networks over two-dimensional mobility terrains. The analytical framework we introduced is based on a special discretization technique, and provided the long-run location and speed characteristics in full generality for a limited version of the model proposed where mobiles are only allowed to move towards one of the finite number of available directions. We conjectured the long-run distributions of the exact mobility formulation, where mobiles can move at any direction, from the analysis of this limited case. We also examined the correctness of our conjectures for a number of scenarios including random waypoint mobility model and a variant of it where the distribution of speed selected for a movement epoch is dependent on the distance that is going to be traveled.

From application of the results to random waypoint mobility model we derived an approximation to the long-run location distribution over rectangular mobility regions. We validated the accuracy of the approximation by simulation, and after comparing the marginals with proven results for one-dimensional regions pointed out that accuracy is insensitive to proportion between the dimensions of the rectangular region. In addition, we showed the applicability of the mobility framework and its corresponding analysis to a mobility terrain where mobiles are restricted to move on predefined paths, and obtained the long-run location distributions in closed form expressions. Our analysis and example scenarios indicate that rich mobility models can be efficiently brought into the analytical studies concentrating performance characteristics of wireless ad hoc networks.

Appendix I

Formulation of $k(x)$ for Example 1

$$k(x)=\begin{cases} k_1(x)+k_4(x)+k_6(x)+k_8(x), & 0<x_1<\frac{a_1}{2}, 0<x_2<\frac{a_2 x_1}{a_1} \\ k_1(x)+k_4(x)+k_6(x)+k_8(x), & \frac{a_1}{2}<x_1<a_1, \\ & 0<x_2<a_2(1-\frac{x_1}{a_1}) \\ k_2(x)+k_4(x)+k_5(x)+k_8(x), & 0<x_1<\frac{a_1}{2}, \\ & \frac{a_2 x_1}{a_1}<x_2<a_2(1-\frac{x_1}{a_1}) \\ k_1(x)+k_3(x)+k_6(x)+k_7(x), & \frac{a_1}{2}<x_1<a_1, \\ & a_2(1-\frac{x_1}{a_1})<x_2<\frac{a_2 x_1}{a_1} \\ k_2(x)+k_3(x)+k_5(x)+k_7(x), & 0<x_1<\frac{a_1}{2}, \\ & a_2(1-\frac{x_1}{a_1})<x_2<a_2 \\ k_2(x)+k_3(x)+k_5(x)+k_7(x), & \frac{a_1}{2}<x_1<a_1, \frac{a_2 x_1}{a_1}<x_2<a_2 \end{cases}, \tag{85}$$

where $k_i(x)$, $i=1,\ldots,8$ are formulated by the equations in (86,87,...,93) that are located at the bottom of the page.

APPENDIX II

Proof of Lemma 1

Proof: If the integral equation (9) has a unique solution, then $\varphi_i > 0$ for all $i = 0,\ldots,n-1$. Hence, the states of the form $(c_i, 0)$ will be visited eventually, and in order to satisfy irreducibility, it is enough to verify the reachability to the states of the form $(c_i, c_j, z_r, 1)$ from the state $(c_i, 0)$. Clearly this can be satisfied only if $\nu_{r|i,j} > 0$ for all possible choices of r, i, and j.

Thus, if the conditions we listed above for irreducibility holds, then all states are periodic with the same period, or else all states are aperiodic. For some finite parameters of n and m, where $n > 1$ and $m > 1$, if generate all of the states in the state space $\mathcal{S}$, and concentrate on the state $(c_0, c_1, z_r, 1)$, then we can easily show that it is possible to return back to $(c_0, c_1, z_r, 1)$ in four or seven transitions after leaving it. Since the greatest common divisor of them is 1, the state $(c_0, c_1, z_r, 1)$ becomes aperiodic, and proof completes. ■

Proof of Lemma 2

Proof: The proof is by direct substitution. First, according to the transitions given in Table I, notice that only the states of the form $(c_i, c_j, z_r, 1)$, where $c_j \in n_h(c_i)$ (also $c_i \in n_h(c_j)$), makes a transition to the states $(c_j, 0)$. Hence, observe for a given $c_j \in \tilde{R}$ that

$$\sum_{\substack{c_i\in\tilde{R},\\ c_i\in n_h(c_j)}} \boldsymbol{\pi}_{i,j}^{(d)} e_m = \sum_{\substack{c_i\in\tilde{R},\\ c_i\in n_h(c_j)}} \Big(\sum_{c_{i'}\in p_{t,1}^{(d)}(i,j)} \varphi_{i'}\tau_{j|i'} + \frac{1}{2} \sum_{c_{i'}\in p_{t,2}^{(d)}(i,j)} \varphi_{i'}\tau_{j|i'} \Big)/N \tag{94}$$

Now, for all $c_{i^*} \in n_h(c_j)$, each member of the set $p_{t,2}^{(d)}(i^*, j)$ will be also a member of one more set denoted by $p_{t,2}^{(d)}(i^{**}, j)$ for a different $c_{i^{**}} \in n_h(c_j)$. Also, for every c_{i^*}, $c_{i^{**}} \in n_h(c_j)$, $p_{t,1}^{(d)}(i^*, j) \cap p_{t,1}^{(d)}(i^{**}, j) = \{\}$. Hence, we get the following for the above equality:

$$\begin{aligned} \sum_{\substack{c_i\in\tilde{R},\\ c_i\in n_h(c_j)}} \boldsymbol{\pi}_{i,j}^{(d)} e_m &= \sum_{c_{i'}\in\tilde{R}} \varphi_{i'}\tau_{j|i'}/N - \varphi_j\tau_{j|j}/N \\ &= (\varphi_j - \varphi_j\tau_{j|j})/N \\ &= \pi_j^{(d)} \end{aligned} \tag{95}$$

Now, it remains to concentrate on the transitions to the states of the form $(c_i, c_j, z_r, 1)$. According to Table I, the states of the form $(c_i, 0)$, and the states $(c_{i'}, c_j, z_r, 1)$, where $c_{i'} \in p_{t,1}^{(d)}(i, j) \cap n_h(c_i)$, make a transition to the state $(c_i, c_j, z_r, 1)$

$$k_1(x) = \frac{(a_1-x_1)\,x_2\left[2\,a_2\,x_1 + a_1\,(x_1-x_2) + x_1\,x_2\log(\frac{x_1(a_2-x_2)}{(a_1-x_1)x_2})\right]}{2\,a_1^2\,a_2^2\,x_1} \tag{86}$$

$$k_2(x) = \frac{x_1\,(a_2-x_2)\left[2\,a_1\,x_2 + a_2\,(x_2-x_1) + x_1\,x_2\log(\frac{(a_1-x_1)x_2}{x_1(a_2-x_2)})\right]}{2\,a_1^2\,a_2^2\,x_2} \tag{87}$$

$$k_3(x) = \frac{(a_1-x_1)\,(a_2-x_2)\left[a_2\,(x_1-a_1) + x_2\,(a_2+2a_1) + (a_1-x_1)\,x_2\log(\frac{x_1\,x_2}{(a_1-x_1)(a_2-x_2)})\right]}{2\,a_1^2\,a_2^2\,x_2} \tag{88}$$

$$k_4(x) = \frac{x_1\,x_2\left[(a_1+2\,a_2)\,(a_1-x_1) - a_1\,x_2 + (a_1-x_1)\,x_2\log(\frac{(a_1-x_1)(a_2-x_2)}{x_1\,x_2})\right]}{2\,a_1^2\,a_2^2\,(a_1-x_1)} \tag{89}$$

$$k_5(x) = \frac{x_1\,(a_2-x_2)\left[a_1\,(a_1-x_1+x_2) + a_2\,(a_1-2x_1) + (a_1-x_1)\,(a_2-x_2)\log(\frac{(a_1-x_1)x_2}{x_1(a_2-x_2)})\right]}{2\,a_1^2\,a_2^2\,(a_1-x_1)} \tag{90}$$

$$k_6(x) = \frac{(a_1-x_1)\,x_2\left[a_2\,(a_1+a_2+x_1) - (2\,a_1+a_2)\,x_2 + (a_1-x_1)\,(a_2-x_2)\log(\frac{x_1(a_2-x_2)}{(a_1-x_1)x_2})\right]}{2\,a_1^2\,a_2^2\,(a_2-x_2)} \tag{91}$$

$$k_7(x) = \frac{(a_1-x_1)\,(a_2-x_2)\left[2\,a_2\,x_1 + a_1\,(x_1+x_2-a_2) + x_1\,(a_2-x_2)\log(\frac{x_1\,x_2}{(a_1-x_1)(a_2-x_2)})\right]}{2\,a_1^2\,a_2^2\,x_1} \tag{92}$$

$$k_8(x) = \frac{x_1\,x_2\left[a_2\,(2\,a_1+a_2-x_1) - (2\,a_1+a_2)\,x_2 + x_1\,(a_2-x_2)\log(\frac{(a_1-x_1)(a_2-x_2)}{x_1\,x_2})\right]}{2\,a_1^2\,a_2^2\,(a_2-x_2)} \tag{93}$$

with a nonzero probability, given their discrete speed matches. Furthermore, the states of the form $(c_{i'}, c_j, z_r, 1)$, where $c_{i'} \in p_{t,2}^{(d)}(i,j) \cap n_h(c_i)$, jump to state $(c_i, c_j, z_r, 1)$ with probability 1/2. Similar to other case, the component for speed must also match.

It can be easily observed that, the set $p_{t,1}^{(d)}(i,j) \cap n_h(c_i)$ is either empty or have only one element. Similarly, the set $p_{t,2}^{(d)}(i,j) \cap n_h(c_i)$, is either empty or have two elements. Without loss of generality, let c_{i_1} denote the only member of $p_{t,1}^{(d)}(i,j) \cap n_h(c_i)$, and let c_{i_2} and c_{i_3} denote the only two members of $p_{t,2}^{(d)}(i,j) \cap n_h(c_i)$. Now, observe the following:

$$\bigcup_{i^* \in \{i_1,i_2,i_3\}} p_{t,1}^{(d)}(i^*,j) = p_{t,1}^{(d)}(i,j) - \{c_i\} \quad (96)$$

$$\bigcup_{i^* \in \{i_1,i_2,i_3\}} p_{t,2}^{(d)}(i^*,j) = p_{t,2}^{(d)}(i,j) \quad (97)$$

In view of these discussions, observe the following:

$$\begin{aligned}
&\pi_i^{(d)} \frac{\tau_{j|i}}{1-\tau_{i|i}} \boldsymbol{\nu}_{m|i,j} + \sum_{c_{i'} \in p_{t,1}^{(d)}(i,j) \cap n_h(c_i)} \boldsymbol{\pi}_{i',j}^{(d)} \\
&+(1/2) \sum_{c_{i'} \in p_{t,2}^{(d)}(i,j) \cap n_h(c_i)} \boldsymbol{\pi}_{i',j}^{(d)} \\
&= \varphi_i \tau_{j|i} \boldsymbol{\nu}_{m|i,j}/N + \sum_{c_{i'} \in p_{t,1}^{(d)}(i,j)} \varphi_{i'} \tau_{j|i'} \boldsymbol{\nu}_{m|i',j}/N \\
&\quad -\varphi_i \tau_{j|i} \boldsymbol{\nu}_{m|i,j}/N + \frac{1}{2} \sum_{c_{i'} \in p_{t,2}^{(d)}(i,j)} \varphi_{i'} \tau_{j|i'} \boldsymbol{\nu}_{m|i',j}/N \\
&= \boldsymbol{\pi}_{i,j}^{(d)} \qquad (98)
\end{aligned}$$

which concludes the proof. ■

Proof of Claim 1

Proof: First, observe the following simplification for $\hat{D}_n^{(d)}$:

$$\hat{D}_n^{(d)} = E[\frac{1}{V^*}] \sum_{c_i \in \tilde{R}} \Big(\sum_{c_j \in \tilde{R} - \{c_i\}} \Big(\sum_{c_{i'} \in p_{t,1}^{(d)}(i,j)} \varphi_{i'} \tau_{j|i'} + \frac{1}{2} \sum_{c_{i'} \in p_{t,2}^{(d)}(i,j)} \varphi_{i'} \tau_{j|i'} \Big) \Big) \Delta c^{(d)}, \quad (99)$$

Now in order to prove our claim, given the cells $c_{i^*}, c_{j^*} \in \tilde{R}$, we have to identify how many times the expression $\varphi_{i^*} \tau_{j^*|i^*}$ appears in the expanded version of the triple summation given above. For this purpose, let $path_1^{(d)}(i^*,j^*)$ and $path_2^{(d)}(i^*,j^*)$ denote the cells that are located on the path $\tilde{p}^{(d)}(i^*,j^*)$ with probabilities 1 and $1/2$, respectively. Furthermore, let n_1 and n_2 denote the cardinalities of those sets. Obviously, n_2 is even, and $n_1 + n_2/2 = dis(i^*,j^*)$.

With respect to these notations, observe that if we expand the triple summation given above, there will be terms where the index of the outermost summation is a member of either the set $path_1^{(d)}(i^*,j^*)$, or the set $path_2^{(d)}(i^*,j^*)$, and the index of the middle summation is c_{j^*}. Moreover, if $c_{i'} \in path_1^{(d)}(i^*,j^*)$, then $c_{i^*} \in p_{t,1}^{(d)}(i',j^*)$. Therefore, since there are n_1 different cells in the $path_1^{(d)}(i^*,j^*)$, the expression $\varphi_{i^*} \tau_{j^*|i^*}$ will appear n_1 times in the expanded summation. Similarly, for all $c_{i''} \in p_{t,2}^{(d)}(i^*,j^*)$, the expression $(1/2)\varphi_{i^*} \tau_{j^*|i^*}$ will appear in the expanded summation. As a result, $\varphi_{i^*} \tau_{j^*|i^*}$ appears in the summation for $n_1 + n_2/2$ times, which is equal to $dis(i^*,j^*)$, and proof completes. ■

Proof of Theorem 1

Proof: To prove $F_{X^{(d)}}(x,a,b)$ in (32) we first define the discretisized version of it according to the parameters n, m, and take the limit of the resulting expression as n and m approach infinity. Hence, let c_i, which can be a square or a hexagon on the discretisized region, also denote the region bounded by it. Also, for a given $R^{(d)}(x,b)$, let $\tilde{R}^{(d)}(x,b)$ denote the cells in $\tilde{R}$ where each c_i belonging to it satisfies the condition $c_i \subset R^{(d)}(x,b)$. Additionally, for the rest of this proof we will use the notations $\tilde{R}^{(d)}(a)$ and $\tilde{R}$ (i.e., the set of cells covering the discretisized region) interchangeably.

Now for a given $R^{(d)}(a)$, and $R^{(d)}(x,b) \subseteq R^{(d)}(a)$, using the formulation of $p_i^{(d)}$ in (20) (i.e., long-run proportion of time that terminal stays in cell c_i), we define

$$\begin{aligned}
&F_{X^{(d)}}^{(n,m)}(x,a,b) \\
&= \frac{\sum_{c_i \in \tilde{R}^{(d)}(x,b)} \varphi_i (1-\tau_{i|i}) E[T_{p_i}] + \sum_{r=1}^{m} \sum_{c_i \in \tilde{R}^{(d)}(x,b)} k_{i,r}^{(d)}}{N_{n,m}^{(d)}}, \quad (100)
\end{aligned}$$

Now, let $K_n^{(d)}(x,z_r,b,a) = \sum_{c_i \in \tilde{R}^{(d)}(x,b)} k_{i,r}^{(d)}$. Hence, according to the definition of $k_{i,r}^{(d)}$ in (22) we get

$$\begin{aligned}
K_n^{(d)}(x,z_r,b,a) =& \sum_{c_i \in \tilde{R}^{(d)}(x,b)} \sum_{c_j \in \tilde{R} - \{c_i\}} \Big(\sum_{c_{i'} \in p_{t,1}^{(d)}(i,j)} \varphi_{i'} \tau_{j|i'} \frac{1}{z_r} \nu_{r|i',j} \\
&+ \frac{1}{2} \sum_{c_{i'} \in p_{t,2}^{(d)}(i,j)} \varphi_{i'} \tau_{j|i'} \frac{1}{z_r} \nu_{r|i',j} \Big) \Delta c^{(d)}, \quad (101)
\end{aligned}$$

Next, for a given $c_i \in \tilde{R}^{(d)}(x,b)$, $c_j \in \tilde{R} - \{c_i\}$, and $c_{i'} \in p_{t,1}^{(d)}(i,j)$, it can be easily shown that, if $\ell(p,i',j)$, where $p = 1$, denotes the number of discrete jumps done over the region $R^{(d)}(x,b)$ while moving from $c_{i'}$ to c_j, then $c_{i'}$ will also be a member of other $\ell(1,i',j) - 1$ many $p_{t,1}^{(d)}(i,j)$ generated for all different $c_i \in \tilde{R}^{(d)}(x,b)$ and located on the path from $c_{i'}$ to c_j. Hence, the expression $\varphi_{i'} \tau_{j|i'} \frac{1}{z_r} \nu_{r|i',j} \Delta c^{(d)}$ will appear $\ell(1,i',j)$ times in the expansion of the triple summation above. Obviously, the same statement can be also constructed by first considering a $c_{i'} \in p_{t,2}^{(d)}(i,j)$, and making the rest of the statements according to $\ell(1/2,i',j)$. As a result, $K_n^{(d)}(x,z_r,b,a)$ would be equivalent to the following.

$$\begin{aligned}
&K_n^{(d)}(x,z_r,b,a) \\
&= \sum_{c_j \in \tilde{R}^{(d)}(a)} \Big(\sum_{c_{i'} \in S_n^{(d)}(1,j,x,b)} \varphi_{i'} \tau_{j|i'} \frac{1}{z_r} \nu_{r|i',j} \ell(1,i',j)\, \Delta c^{(d)} \\
&\quad + \frac{1}{2} \sum_{c_{i'} \in S_n^{(d)}(1/2,j,x,b)} \varphi_{i'} \tau_{j|i'} \frac{1}{z_r} \nu_{r|i',j} \ell(1/2,i',j)\, \Delta c^{(d)} \Big) \quad (102)
\end{aligned}$$

where $S_n^{(d)}(p,j,x,b)$ denotes the subset of cells in $\tilde{R}^{(d)}(a)$ where $\forall\, c_{i'} \in S_n^{(d)}(p,j,x,b)$ the movement epoch between $c_{i'}$

and c_j passes through the region $R^{(d)}(x,b)$ with probability p.

At this point, we note that $K_n^{(d)}(x,z_r,b,a)$ is actually the discretisized version of $K^{(d)}(x,v,b,a)$. Therefore, in order to make a formal transition from (102) to (34) observe the following substitutions for sufficiently high values of n and m:

$$\varphi_{i'} = f_{X_s}(x_{i'}^*)\,\Delta A, \quad (103)$$

$$\tau_{j|i'} = f_{X_d|X_s}(x_j^*|X_S \in c_{i'})\,\Delta A, \quad (104)$$

$$\nu_{r|i',j} = f_{V|X_s,X_d}(v_r^*|X_s \in c_{i'}, X_d \in c_j)\,\Delta v \quad (105)$$

where ΔA denote the area covered by cell c_i, and the numbers $x_{i'}^*$, x_j^*, and v_r^* are chosen arbitrarily within the subregions covered by the cells $c_{i'}$, c_j, and $[r\Delta v, (r+1)\Delta v]$, respectively, for $i', j = 0,\ldots,n-1$, and $r = 1,\ldots,m$.

After inserting the substitutions in (103), (104), and (105) back to the expression in (102), observe first that the term $\ell(p,i',j)\,\Delta c^{(d)}$ converges to $L^{(d)}(p,x_s,x_d,x,b,a)$ (i.e., the total distance traveled over $R^{(d)}(x,b)$ while moving from x_s to x_d, and passing through $R^{(d)}(x,b)$ with probability p) as $n \to \infty$. Clearly, if $c_{i'}$ and c_j are outside $R^{(d)}(x,b)$ then they will be equal for all choices of n. Based on this observation, we can also state that the region bounded by the cells in $S_n^{(d)}(p,j,x,b)$ converges to $S^{(d)}(p,x_d,x,b)$ in (31) as $n \to \infty$. Consequently, the taking the limit $K_n^{(d)}(x,z_r,b,a)$ as $n \to \infty$ ($\Delta A \to 0$) is equivalent to transforming double summation operations over the regions $\tilde{R}^{(d)}(a)$ and $S_n^{(d)}(p,j,x,b)$, into double integration operations over $R^{(d)}(a)$ and $S^{(d)}(p,x_d,x,b)$, respectively. After this transformation, when the limit of the resulting expression is taken as $m \to \infty$, the $K^{(d)}(x,v,b,a)$ given by (34) can be easily obtained. Finally, by substituting φ_i and $\tau_{i|i}$ with $f_{X_s}(x_i^*)\,\Delta A$ and $f_{X_d|X_s}(x_i^*|X_S \in c_i)\,\Delta A$, respectively, it can be immediately observed that

$$\lim_{n\to\infty} \sum_{c_i \in \tilde{R}^{(d)}(x,b)} \varphi_i(1-\tau_{i|i})E[T_{p_i}] = E[T_p|X_s \in R^{(d)}(x,b)]\,\Pr\{X_s \in R^{(d)}(x,b)\} \quad (106)$$

Hence, the limit of $F_{X^{(d)}}^{(n,m)}(x,a,b)$ as $n \to \infty$ and $m \to \infty$ will be equivalent to the $F_{X^{(d)}}(x,a,b)$ given by (32).

In order to prove $f_{\tilde{V}^{(d)}}(\tilde{v})$ (33), we need to take the limit of $\psi_r^{(d)}$ (21) as n and m approaches infinity. Clearly this can be done by summing the terms $K_n^{(d)}(x,z_r,b,a)$ (102) for all $R^{(d)}(x,b) \in \mathcal{S}^{(d)}(a,b)$. Since we have already shown that $K_n^{(d)}(x,z_r,b,a)$ converges to $K^{(d)}(x,v,b,a)$ as $n \to \infty$ and $m \to \infty$, it immediately follows that $f_{\tilde{V}^{(d)}}(\tilde{v})$ can be formulated by summing the $K^{(d)}(x,v,b,a)$ for all $R^{(d)}(x,b) \in \mathcal{S}^{(d)}(a,b)$ and also normalizing it the end, which completes the proof. ■

REFERENCES

[1] D. N. Alparslan and K. Sohraby, "A generalized random mobility model for wireless ad hoc networks and its analysis: One-dimensional case," University of Missouri -Kansas City, School of Computing and Engineering, Kansas City, Missouri, Tech. Rep., Dec. 2004, http://d.web.umkc.edu/dna5a0 (submitted to IEEE/ACM Transactions on Networking).

[2] C. Bettstetter, "Smooth is better than sharp: a random mobility model for simulation of wireless networks," in *Proc. 4th ACM Int. Workshop on Modeling Analysis and Simulation of Wireless and Mobile Systems (MSWiM)*, Rome, Sept. 2001, pp. 19–27.

[3] T. Camp, J. Boleng, and V. Davies, "A survey of mobility models for ad hoc network research," *Wireless Communications & Mobile Computing (WCMC): Special issue on Mobile Ad Hoc Networking: Research, Trends and Applications*, vol. 2, no. 5, pp. 483–502, 2002.

[4] D. B. Johnson and D. A. Maltz, "Dynamic source routing in ad hoc wireless networks," in *Mobile Computing*, Imielinski and Korth, Eds. Dordrecht, The Netherlands: Kluwer Academic Publishers, 1996, vol. 353.

[5] C. Bettstetter, G. Resta, and P. Santi, "The node distribution of the random waypoint mobility model for wireless ad hoc networks," *IEEE Trans. Mobile Computing*, vol. 2, no. 3, pp. 257–269, 2003.

[6] W. Navidi and T. Camp, "Stationary distributions for the random waypoint mobility model," *IEEE Trans. Mobile Computing*, vol. 3, no. 1, pp. 99–108, 2004.

[7] J. Yoon, M. Liu, and B. Noble, "Sound mobility models," in *Proc. ACM MOBICOM*, San Diego, Sept. 2003, pp. 205–216.

[8] I. F. Akyildiz, Y. B. Lin, W. R. Lai, and R.-J. Chen, "A new random walk model for pcs networks," *IEEE Trans. Commun.*, vol. 18, no. 7, pp. 1254 – 1260, 2000.

[9] I. F. Akyildiz, J. S. M. Ho, and Y. B. Lin, "Movement-based location update and selective paging for pcs networks," *IEEE/ACM Trans. Networking*, vol. 4, no. 4, pp. 629 – 638, 1996.

[10] E. Çinlar, *Introduction to Stochastic Processes*. Prentice-Hall Inc., 1975, ch. 10.

[11] W. Feller, *An Introduction to Probability Theory and Its Applications*, 2nd ed. Wiley, 1970, vol. II, ch. 6.

[12] T. H. Cormen, C. E. Leiserson, and R. L. Rivest, *Introduction to Algorithms*. The MIS press, 1989, ch. 35.

[13] W. B. Davenport, *Probability and Random Processes*. McGraw-Hill, 1970, ch. 5.

[14] P. J. Davis and P. Rabinowitz, *Methods of Numerical Integration*, 2nd ed. Academic Press, 1983, ch. 1,5.

[15] M. Abramowitz and I. A. Segun, Eds., *Handbook of Mathematical Functions*. Dover Publications, 1970, ch. 25.

[16] D. M. Blough, G. Resta, and P. Santi, "A statistical analysis of the long-run node spatial distribution in mobile ad hoc networks," in *Proc. 5th ACM Int. Workshop on Modeling Analysis and Simulation of Wireless and Mobile Systems (MSWiM)*, Atlanta, Sept. 2002, pp. 30–37.

[17] C. Bettstetter and C. Wagner, "The spatial node distribution of the random waypoint mobility model for wireless ad hoc networks," in *Proc. First German Workshop Mobile Ad-Hoc Networks (WMAN)*, 2002, pp. 41–58.

[18] N. L. Johnson and S. Kotz, *Continuous Univariate Distributions-1*. Houghton Mifflin, 1970, vol. I, ch. 13.

[19] F. Bai, N. Sadagopan, and A. Helmy, "Important: A framework to systematically analyze the impact of mobility on performance of routing protocols for adhoc networks," in *Proc. IEEE INFOCOM*, San Francisco, Mar. 2003.